



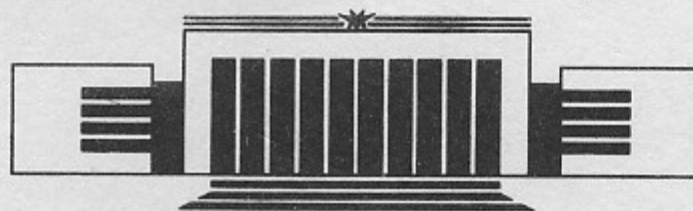
33

ИНСТИТУТ ЯДЕРНОЙ ФИЗИКИ СО АН СССР

V.I. Telnov

**PROBLEMS OF OBTAINING  
 $\gamma\gamma$  AND  $\gamma e$  COLLIDING BEAMS  
AT LINEAR COLLIDERS**

**PREPRINT 89-90**



НОВОСИБИРСК

Problems of Obtaining  
 $\gamma\gamma$  and  $\gamma e$  Colliding Beams  
at Linear Colliders<sup>\*)</sup>

V.I. Telnov

Institute of Nuclear Physics  
630090, Novosibirsk 90, USSR

ABSTRACT

Physical principles of colliding  $\gamma\gamma$ - and  $\gamma e$ -beams are described briefly. Beam-beam effects restricting luminosity are considered. A possible schemes of collision and beam ejection are discussed, together with associated problems. Requirements for accelerator and laser parameters are formulated. Estimation of attainable luminosities and examples of physical processes are given.

<sup>\*)</sup> Report at Intern. Workshop on Next Generation Linear Colliders, December 1988, Stanford, SLAC, USA.

Contents

1. Introduction . . . . .	5
2. General Features of Linear $e^+e^-$ -Colliders . . . . .	6
3. Two Photon Physics at $e^+e^-$ Storage Rings . . . . .	11
4. Methods of $e \rightarrow \gamma$ Conversion at Linear Colliders . . . . .	11
5. Backward Compton Scattering . . . . .	14
6 Scheme of $\gamma\gamma$ -, $\gamma e$ -Collisions . . . . .	23
7. Beam-Collision Effects. . . . .	24
8. Removal of Photons and Electrons from the Conversion and Interaction Regions . . . . .	35
9. Final Focusing . . . . .	42
10. Luminosity, Monochromaticity . . . . .	46
11. Characteristic Cross Sections of Processes. . . . .	50
Conclusion. . . . .	52

NOVOSIBIRSK  
1989

## 1. INTRODUCTION

It is well known that due to severe synchrotron radiation in storage rings, future  $e^+e^-$ -colliders in the TeV energy region will be linear. The Soviet Union is planning a linear collider VLEPP [1], designed at Novosibirsk to be constructed at Protvino. Similar projects are under development now at CERN (CLIC) [2], SLAC (TLC) [3], KEK (JLC) [4].

The general parameters of these colliders (according to present expectations) are shown in Table 1.

Table 1

	VLEPP	CLIC	TLC	JLC
Beam energy (TeV)	1	1	0.5	0.5
Luminosity ( $\text{cm}^{-2}\text{s}^{-1}$ )	1	1.1	6.2	1
Length (km)	20	25(13)	7.3	10
Accel. grad (MeV/m)	100	80(160)	186	100
Particle/bunch ( $10^{10}$ )	20	0.54	1.4	1.9
Rep. rate (kHz)	0.1	5.8	0.36	0.51
Num. of bunch.	1	1	10	3
Beamstrah. $\delta$ (%)	10	19	10	5
$R = \sigma_x/\sigma_y$	150	1	132	1
$\sigma_y$ ( $\mu\text{m}$ )	0.02	0.065	0.003	0.17
$\sigma_z$ (mm)	0.75	0.3	0.07	1.0

Unlike the situation in storage rings, in linear colliders each bunch is used only once. This makes possible the use of electrons for production of high energy photons to obtain colliding  $\gamma\gamma$ - and  $\gamma e$ -beams. This idea was put forward by the author and colleagues in Ref. [5]. Further discussion of this subject were presented in Refs [6—11, 41]. It was shown that using the designed linear colliders one can obtain  $\gamma\gamma$ ,  $\gamma e$  colliding beams with high energy and luminosity. The required high energy photons were suggested to be obtained by backward Compton scattering of laser light on the electron beams of colliders. This method is well known [17]. Small beam sizes in linear colliders make it possible to achieve a conversion coefficient (number of high energy photons per one electron)  $k \sim 1$  at the moderate laser flush energy of  $\sim 10$  J. The modern level of laser techniques should allow one to build a laser with all required parameters, although special development is necessary.

If it can be realized,  $\gamma\gamma$ - and  $\gamma e$ -collisions could considerably increase the potentialities of  $e^+e^-$ -colliders. Many interesting processes can be investigated in these collisions [12—13]. Note, that physics in  $\gamma\gamma$ - and  $\gamma e$ -collisions at TeV energies has been studied theoretically much less than in  $e^+e^-$ -reactions.

In this paper a review of physical principles of colliding  $\gamma\gamma$ - and  $\gamma e$ -beams is given. Beam collision effects restricting the  $\gamma\gamma$ - and  $\gamma e$ -luminosities are examined for the first time as well as a proposed scheme of collisions and removal of disrupted beams and associated problems. Requirements on accelerator and laser parameters are formulated, and estimates of attainable  $\gamma\gamma$ - and  $\gamma e$ -luminosities are presented for planned linear colliders.

## 2. GENERAL FEATURES OF LINEAR $e^+e^-$ -COLLIDERS

Let us consider briefly the most essential features of  $e^+e^-$  linear colliders and inherent problems. Since  $\gamma\gamma$ -,  $\gamma e$ -beams are produced in  $e^+e^-$ -accelerators there are some common problems. But in some aspects, for example, beam-beam effects, there are considerable differences. This short excursion enables us to realize better an initial picture, and it will be easier further to orient ourselves in the problems under discussion, to evaluate possible advantages of different methods.

## 2.1. Accelerating Gradient

For «warm» accelerating structures at the wave length of a few centimeters a gradient of 100—200 MeV/m can be achieved. For superconducting structures, which allows energy recovery at high repetition rates, the obtained fields are much lower.

## 2.2. Repetition Rate

As one can see from the Table 1, the repetition rate varies from 0.1 to 5 kHz. It is determined mainly by available RF power and also by the time needed for preparation of beams with small emittances. For increasing effective rate a multibunching mode of operation is foreseen for some projects. It can be done when one beam takes away a small part of the RF energy.

## 2.3. Beam Size at the Interaction Region

Due to low repetition rate (in comparison with storage rings) a very small beam cross section is required. The luminosity of colliders is

$$L = \frac{N^2 f}{S}, \quad (2.1)$$

where  $N$ —number of particles in a bunch and  $S = 4\pi\sigma_x\sigma_y$ . For example for obtaining  $L = 10^{33} \text{ cm}^{-2}\text{s}^{-1}$  at VLEPP ( $N = 2 \cdot 10^{11}$  and  $f = 100 \text{ Hz}$ ) beam cross section of  $S = 4 \cdot 10^{-9} \text{ cm}^2$  is needed.

Transverse beam size is determined by the emittance  $\epsilon$ . Near by the interaction region the r.m.s. size of a bunch depends on the coordinate  $z$  along the beam as follows ( $i \equiv x, y$ )

$$\sigma_i(z) = \sigma_i \sqrt{1 + \frac{z^2}{\beta_i^2}}, \quad (2.2)$$

where  $\beta_i$  is the beta function. From here the emittance  $\epsilon_i = \sigma_i \sigma_i' = \sigma_i^2 / \beta_i$  and the beam size in the focus

$$\sigma_i = \sqrt{\epsilon_i \beta_i}. \quad (2.3)$$

The luminosity grows with decreasing of  $\beta$  up to  $\sigma_z$  and almost does not change further. With increasing energy the emittance of the bunch decreases:  $\epsilon_i = \epsilon_{ni} / \gamma$ , where  $\epsilon_{ni}$  is the normalized emit-

tance,  $\gamma = E_0/mc^2$ . The beams with small  $\varepsilon_{ni}$  are prepared in damping rings.

#### 2.4. Beam-Beam Effects, Ultimate Luminosity

Due to small beam sizes particles are exposed to a very strong electromagnetic field created by the opposing beam. This leads to the following two effects:

1. Particles emit synchrotron radiation which is called «beamstrahlung». Beamstrahlung reduces the mean electron energy and increases the energy spread.

2. At some conditions beam instabilities arise and the luminosity drops. When the beam density is close to the critical one some enhancement of the luminosity relative to the geometrical one is expected (pinch effect).

Both these effects impose principal restrictions on the attainable  $e^+e^-$ -luminosity.

In the first case a drastic gain is given by flat beams [14]. The field in the beam is proportional to  $1/\sigma_x \propto \sqrt{L/R}$ , where  $R = \sigma_x/\sigma_y$  is the ratio of the transverse beam sizes (aspect ratio),  $\sigma_x$ —larger size. From here follows, that at a given relative energy loss, number of particles and beam length the luminosity is linearly proportional to  $R$ .

In the classical beamstrahlung regime, i. e. when critical energy  $\omega_c \ll E$ , the mean relative energy losses are equal [14]

$$\delta \approx \frac{5N^2 r_e^3 \gamma}{6\sigma_z \sigma_y^2 (1+R)^2}, \quad (2.4)$$

where  $r_e = e^2/mc^2 = 2.8 \cdot 10^{-13}$  cm is the classical radius of electron. Hence, the maximum luminosity at the losses  $\delta$  and aspect ratio  $R \gg 1$

$$L \simeq 2.2 \cdot 10^{30} R \delta f H_y E_0 (\text{TeV}) \sigma_z (\text{cm}), \text{ cm}^{-2} \text{s}^{-1}, \quad (2.5)$$

or at optimal focusing ( $\beta_y = \sigma_z$ )

$$L \approx \frac{0.1 N f H_y}{r_e^2} \left( \frac{\delta r_e}{\varepsilon_{ny}} \right)^{1/2}, \quad (2.6)$$

where  $H_y \sim 1-2$  is the pinch factor.

The designed colliders fall within a «transition» regime of radiation (between «classical» and «quantum»). The corresponding parameter is [15]

$$\Upsilon \equiv \frac{2}{3} \frac{\bar{\omega}_c}{E_0} \approx \frac{5N r_e^2 \gamma}{6\alpha(1+R)\sigma_y \sigma_z}, \quad (2.7)$$

where  $\alpha \equiv e^2/\hbar c = 1/137$ .

In the general case [16] the mean relative losses at  $R \gg 1$  are

$$\delta = 3.8\alpha(F_\Upsilon \Upsilon) \sqrt{\frac{L r_e^2}{f R H_y}}, \quad (2.8)$$

where  $F_\Upsilon$  is the function of  $\Upsilon$  ( $F_\Upsilon = 1$  at  $\Upsilon \ll 1$ ). It turns out [15, 16], that  $(F_\Upsilon \Upsilon)$  changes slowly in the range  $\Upsilon = 0.2 \div 100$  and equals to 0.065, 0.1, 0.18, 0.18, 0.11 at  $\Upsilon = 0.1, 0.2, 1, 10, 100$ , respectively. Assuming  $(F_\Upsilon \Upsilon) = 0.15$ , we get

$$L = 7.5 \cdot 10^{29} R f \delta^2 H_y, \text{ cm}^{-2} \text{s}^{-1} \quad (2.9)$$

or

$$L \approx \frac{70 N f \delta H_y}{r_e^2} \left( \frac{\gamma r_e^2}{\varepsilon_{ny} \sigma_z} \right)^{1/2}. \quad (2.10)$$

For VLEPP beams and  $H_y = 2$  one gets  $\Upsilon = 0.15$ ,  $(F_\Upsilon \Upsilon) = 0.08$  and hence,  $L \approx 10^{33} \text{ cm}^{-2} \text{s}^{-1}$  at  $\delta = 0.11$ .

From formulae, presented above, it follows that one can increase the luminosity without limit by decreasing  $\varepsilon_{ny}$  (increasing  $R$ ). However, this is not possible not only for technical reasons, but also due to the appearance of beam-beam instabilities [14]. The corresponding parameter is the mean number of oscillations of an electron during collision

$$n_y = \frac{1}{\sqrt{2\pi}} \left( \frac{r_e N \sigma_z}{\gamma \sigma_x \sigma_y} \right)^{1/2}. \quad (2.11)$$

The instability, which occurs at  $n_y \sim 1$ , determines the attainable luminosity [14]

$$L_{\max} = \frac{\pi N E_0 f}{2e^2 \sigma_z}. \quad (2.12)$$

From here for VLEPP we get  $L \sim 3 \cdot 10^{33} \text{ cm}^{-2} \text{s}^{-1}$ , and twice as much with taking into account the pinch factor  $H_y \simeq 2$ . For obtaining  $\delta = 0.1$  we must have  $R = 1000$ , which is hardly possible.

We see, that due to collision effects, obtaining high luminosity in  $e^+e^-$ -collisions is a difficult problem.

In  $\gamma\gamma$ - and  $\gamma e$ -collisions, some kind of collision effects also take place. However, in  $\gamma\gamma$ -collisions one can obtain higher luminosity, than in  $e^+e^-$ -collisions.

### 2.5. Reproduction of $e^+e^-$ -Beams

In the linear  $e^+e^-$ -colliders a reproduction of beams is necessary. In the VLEPP scheme [18, 19] the beam, after acceleration up to 150–200 GeV, passes an undulator, where it creates photons of 10 MeV energy. These photons incident on a target produce sufficient electrons and positrons to prepare new bunches. Only the hard part of spectrum is used, where particles had a high degree of polarization ( $\sim 65\%$ ). Further these beams are cooled in damping rings. The initial beam after collision at the interaction region is directed to an absorber.

One-fold usage of the beams is a decisive feature for obtaining photon beams. For this goal positrons are not necessary at all, and electrons can be prepared in the usual way. One can have the polarized electrons using a laser source [20].

### 2.6. Backgrounds

Due to the low repetition rate the background at linear  $e^+e^-$ -colliders is a severe problem. At integrated luminosity of  $L=10^{31} \text{ cm}^{-2}$  per one collision more than  $10^6$  background reactions  $\gamma\gamma \rightarrow e^+e^-$ ,  $\gamma e \rightarrow ee^+e^-$  will happen simultaneously (where  $\gamma$  is the synchrotron or virtual (3.1) photon). At  $Y > 1$  the probability of coherent  $e^+e^-$  pair creation by a photon in a field of the opposing beam also become large [37, 38]. The number of such pairs can account for a few percent of beam electrons. Although the angles of produced particles as well as those of the emitted hard photon are small, particles obtain an additional angle in the field of the opposing beam. In head-on collisions these particles can not pass through lenses and will be absorbed near the detector. This will cause a large flux of reflected particles. Most dangerous are neutrons ( $10^9 \text{ neut./J}$  [21]). In this respect TLC project is of interest, where it is proposed to collide particles at a small crossing angle, so that disrupted beams travel outside lenses. Such a method is exceptionally useful at  $Y \gg 1$ , when a lot of soft electrons and positrons are produced.

### 3. TWO PHOTON PHYSICS AT $e^+e^-$ -STORAGE RINGS

Up to now two photon physics was actively investigated at  $e^+e^-$ -storage rings. With good accuracy one can consider that each electron is accompanied by almost real equivalent photon with the probability [22]

$$dn_\gamma = \frac{\alpha}{\pi} \frac{dy}{y} \left(1 - y + \frac{1}{2} y^2\right) \ln \frac{(1-y) q_m^2}{m^2 y^2}, \quad (3.1)$$

$$dn_\gamma \sim 0.035 \frac{d\omega}{\omega} \quad \text{at } \omega \ll E_0, \quad (3.2)$$

where  $y = \omega/E_0$ ,  $q_m^2 = m_p^2$ ,  $p_\perp^2$ ,  $W_{\gamma\gamma}^2$  depending on the process [13]. The spectral luminosities of  $\gamma e$ - and  $\gamma\gamma$ -collisions are

$$\frac{dL_{\gamma e}}{dz} = L_{e^+e^-} \frac{2\alpha}{\pi} \frac{dz}{z} \left(1 - z^2 + \frac{1}{2} z^4\right) \ln \frac{q_m^2 (1-z^2)}{m^2 z^4}, \quad (3.3)$$

$$\begin{aligned} \frac{dL_{\gamma\gamma}}{dz} = L_{e^+e^-} \frac{2\alpha^2}{\pi^2 z} \left\{ \left[ 2 \left(1 + \frac{z^2}{2}\right)^2 \ln \frac{1}{z} - \right. \right. \\ \left. \left. - \frac{1}{2} (1-z^2) (3+z^2) \right] \ln^2 \left( \frac{q_m^2}{m^2 z^2} \right) - \frac{8}{3} \ln^3 \frac{1}{z} \right\}, \quad (3.4) \end{aligned}$$

where  $z = W_{\gamma e}/2E_0$  for  $\gamma e$  and  $z = W_{\gamma\gamma}/2E_0$  for  $\gamma\gamma$ . The graphs of these functions (and their integrals) are presented in Fig. 1. The integrated gamma-gamma luminosity for the region  $W_{\gamma\gamma}/2E_0 > 0.5$  account for  $L_{\gamma\gamma} \approx 0.4 \cdot 10^{-3} L_{e^+e^-}$ . It is seen that the luminosity of equivalent photons is high enough only for small  $z$  and is much smaller than  $L_{e^+e^-}$  for  $z \sim 1$ .

### 4. METHODS OF THE $e \rightarrow \gamma$ CONVERSION AT LINEAR COLLIDERS

At linear colliders the electron bunches are prepared for every collision anew. This allows the conversion of electrons into photons and thus to obtain  $\gamma\gamma$  and  $\gamma e$  colliding beams. Let us consider possible methods of conversion.

#### 4.1. Bremsstrahlung Radiation

The simple and obvious method of hard photon production is bremsstrahlung on a target. When an electron passes through a

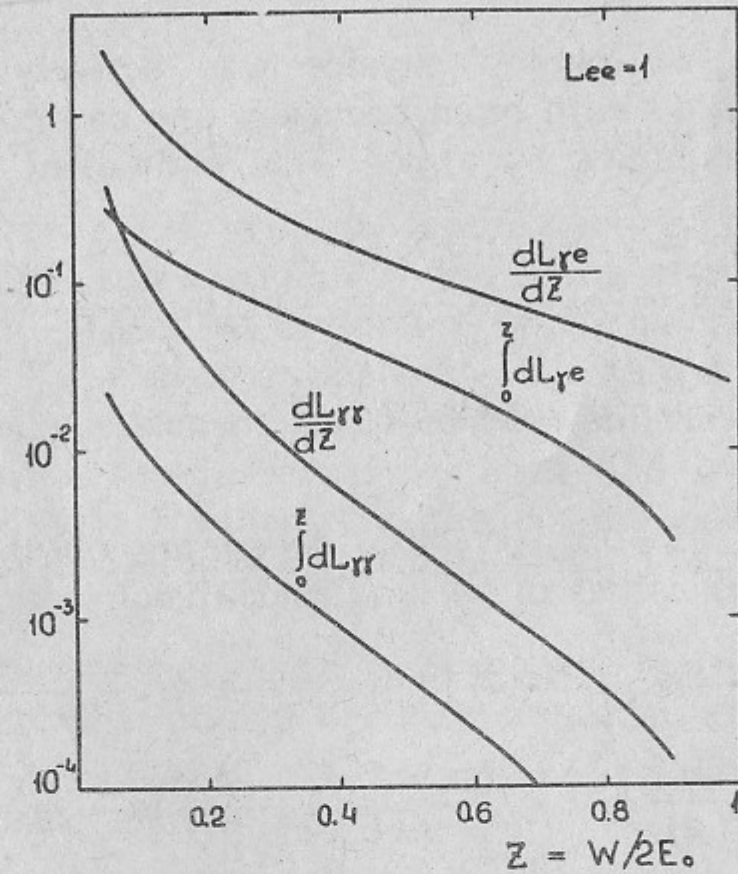


Fig. 1. Spectral luminosity of  $\gamma\gamma$ - and  $\gamma e$ -collisions at  $e^+e^-$ -storage rings.

plate of a thickness  $x$ , the spectrum of emitted photons is

$$dn_\gamma \sim \frac{x}{X_0} \frac{d\omega}{\omega}, \quad (4.1)$$

where  $X_0$  is the radiation length. If we take  $x/X_0=0.35$ , so that the probability of secondary collisions is small, then  $dn_\gamma \sim 0.35 d\omega/\omega$ . We see, that the amount of bremsstrahlung photons is larger than that of virtual photons by one order of magnitude and, hence, the  $\gamma\gamma$ -luminosity will be larger by two orders.

Weak points of this method are:

- a) background due to photonuclear reactions (see below);
- b) soft spectrum of the produced photons.

#### 4.2. The Coherent Bremsstrahlung on Crystals

Unlike the case in an amorphous medium, in crystals a collective interaction of atoms with passing electron takes place [23], resulting in a considerable increase of radiation intensity. The effec-

tive radiation length in a crystal  $X'_0$  can be considerably smaller than  $X_0$  in an amorphous medium. The maximum shortening of the radiation length takes place just at  $E \sim 1$  TeV and the ratio  $X_0/X'_0$  is: for C (diamond) — 168, Si — 80, Ge — 30, W — 11. The spectrum of photons at this energy resembles the usual bremsstrahlung spectrum (4.1).

For our application it is advantageous to choose the crystal with the largest ratio of the radiation length to the photonuclear (ph. n) length. Since  $\sigma_{rad} \propto Z^2 X_0/X'_0$ , and  $\sigma_{ph.n} \sim 0.005 \sigma_n \propto Z^{2/3}$ , then  $\sigma_{rad}/\sigma_{ph.n} \propto Z^{4/3} X_0/X'_0$ . In the extreme cases, diamond and tungsten, these ratios differ only by a factor of two in favour of tungsten.

Let us take a tungsten converter of  $0.3X'_0$  (100  $\mu\text{m}$ ) thickness. Passing the radiator each electron produces  $0.3 \cdot \ln(E/\omega_m)$  photons ( $\omega_m \sim 1$  GeV). The ph. n. collision length in W is about 1000 cm, i. e. the probability of a ph. n. reaction in our converter is of about  $2 \cdot 10^{-5}$ . Hence, one bunch ( $N=2 \cdot 10^{11}$ ) will generate  $\sim 4 \cdot 10^6$  nuclear reaction per crossing. With two bunches and two converters we get more than  $10^7$  reactions per crossing. Evidently, such a level of background is not acceptable.

In the above discussion we neglected electromagnetic processes such as  $e^+e^-$ -production, since particles here have very small angles and are not seen in the detector.

We should not forget also about radiation and heat damage of crystals by such high dense electron beams.

#### 4.3. Beamstrahlung Radiation

At  $\gamma \gg 1$  (eq. (2.7)) the spectrum of beamstrahlung photon becomes hard ( $\bar{\omega} \sim 0.25 E_0$  [15]) and the number of photons is about one per electron ( $n_\gamma \sim 3.78$  at  $\gamma \gg 1$ ). This provides rather high photon-photon luminosity [39]. However, in such an approach the following disadvantages are seen:

- a) a beam-beam instability restricts the luminosity;
- b) many soft particles (both  $e^-$  and  $e^+$ ) are produced and are deflected by the field of the opposing beam in all directions, causing background;
- c) broad spectrum of photons;
- d) in the strong field of the opposing beam, photons will convert into  $e^+e^-$ -pairs (see Sect. 7.1).

#### 4.4. Compton Scattering of Laser Light

If laser light is focussed on an electron beam, the photons after scattering have high energy ( $\omega \sim E_0$ ) and follow along the initial electron direction («backward» Compton scattering [17]). Let us enumerate the main advantages of this method:

- no matter in the beam path;
- the «used» electrons can be swept out from the photon beam;
- in  $\gamma\gamma$ -collisions one can use beams with the cross section smaller than in  $e^+e^-$ -collisions (no beamstrahlung and beam-beam instabilities);
- the photon spectrum is enhanced in the hard region at  $\omega \sim E_0$ , and one can obtain the monochromaticity of collisions  $\Delta W/W \sim 10\%$ .

#### 4.5. Summary of $e \rightarrow \gamma$ Conversion Methods

The Compton scattering has obvious advantages over all other method of  $e \rightarrow \gamma$  conversion considered above. In the following discussions we will consider only this method.

### 5. BACKWARD COMPTON SCATTERING

#### 5.1. Kinematics

Below some useful formulae for Compton scattering are given for the case of interest [7], [10].

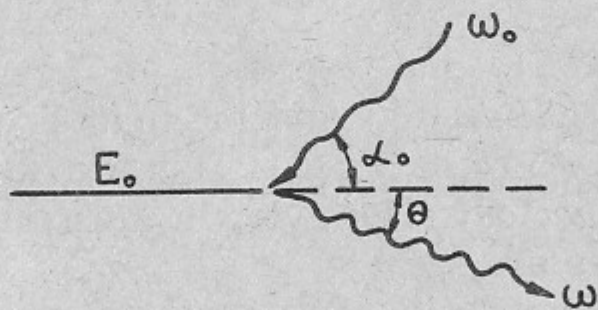


Fig. 2. Kinematics of Compton scattering.

In the conversion region a photon with the energy  $\omega_0$  is scattered on an electron with the energy  $E_0$  at a small collision angle  $\alpha_0$  (Fig. 2). The energy of the scattered photon  $\omega$  depends on its angle  $\theta$  relative to the motion of the incident electron as follows:

$$\omega = \frac{\omega_m}{1 + (\theta/\theta_0)^2}, \quad (5.1)$$

where

$$\omega_m = \frac{x}{x+1} E_0; \quad \theta_0 = \frac{m}{E_0} \sqrt{x+1}; \quad x = \frac{4E_0 \omega_0}{m^2 c^4};$$

$\omega_m$  is the maximum photon energy.

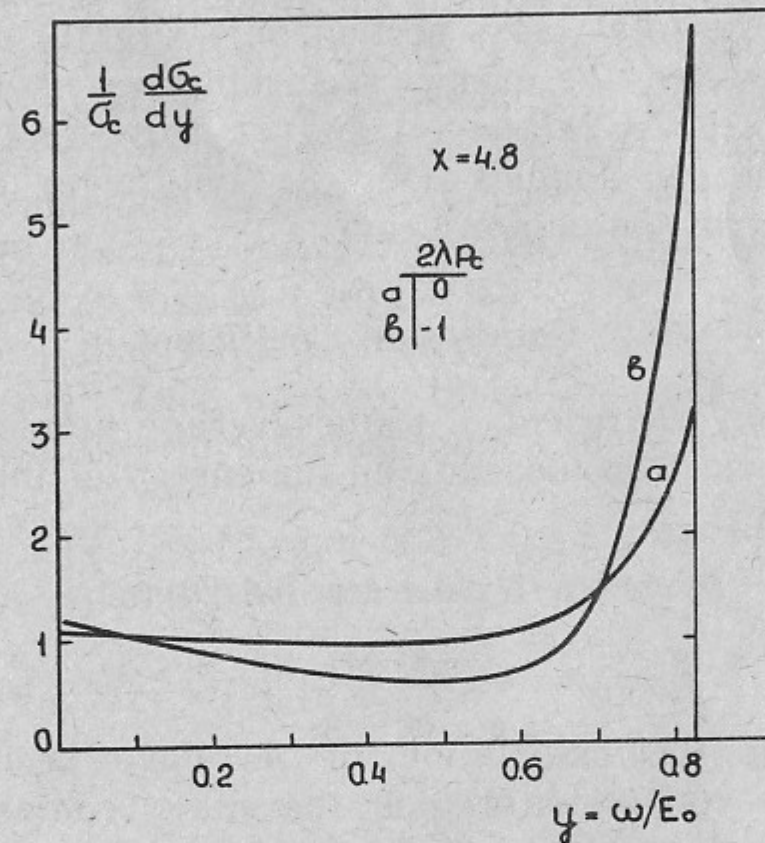


Fig. 3. Energy spectrum of scattered photons.

The energy spectrum of the scattered photons is defined by the cross section (see Fig. 3)

$$\frac{1}{\sigma_c} \frac{d\sigma_c}{dy} \equiv f(x, y) = \frac{2\sigma_0}{x\sigma_c} \left[ \frac{1}{1-y} + 1 - y - 4r(1-r) + 2\lambda P_c r x (1-2r)(2-y) \right],$$

$$y = \frac{\omega}{E_0} \leq y_m = \frac{x}{x+1}, \quad r = \frac{y}{x(1-y)} \leq 1, \quad (5.2)$$

$$\sigma_0 = \pi \left( \frac{e^2}{mc^2} \right)^2 = 2.5 \cdot 10^{-25} \text{ cm}^2.$$

For the polarized beams the spectrum only varies if both electron mean helicity ( $\lambda$ ) and that of the laser photons ( $P_c$ ) are nonzero. The total Compton cross section is



#### 4.4. Compton Scattering of Laser Light

If laser light is focussed on an electron beam, the photons after scattering have high energy ( $\omega \sim E_0$ ) and follow along the initial electron direction («backward» Compton scattering [17]). Let us enumerate the main advantages of this method:

- no matter in the beam path;
- the «used» electrons can be swept out from the photon beam;
- in  $\gamma\gamma$ -collisions one can use beams with the cross section smaller than in  $e^+e^-$ -collisions (no beamstrahlung and beam-beam instabilities);
- the photon spectrum is enhanced in the hard region at  $\omega \sim E_0$ , and one can obtain the monochromaticity of collisions  $\Delta W/W \sim 10\%$ .

#### 4.5. Summary of $e \rightarrow \gamma$ Conversion Methods

The Compton scattering has obvious advantages over all other method of  $e \rightarrow \gamma$  conversion considered above. In the following discussions we will consider only this method.

### 5. BACKWARD COMPTON SCATTERING

#### 5.1. Kinematics

Below some useful formulae for Compton scattering are given for the case of interest [7], [10].

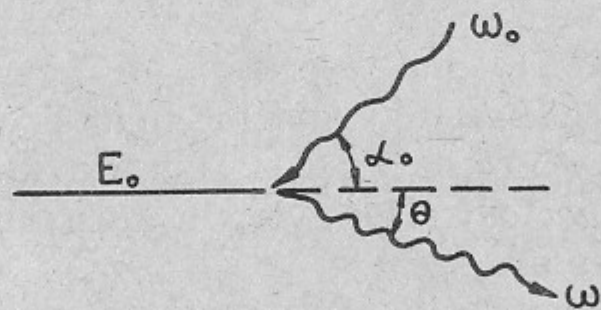


Fig. 2. Kinematics of Compton scattering.

In the conversion region a photon with the energy  $\omega_0$  is scattered on an electron with the energy  $E_0$  at a small collision angle  $\alpha_0$  (Fig. 2). The energy of the scattered photon  $\omega$  depends on its angle  $\theta$  relative to the motion of the incident electron as follows:

$$\omega = \frac{\omega_m}{1 + (\theta/\theta_0)^2}, \quad (5.1)$$

where

$$\omega_m = \frac{x}{x+1} E_0; \quad \theta_0 = \frac{m}{E_0} \sqrt{x+1}; \quad x = \frac{4E_0 \omega_0}{m^2 c^4};$$

$\omega_m$  is the maximum photon energy.

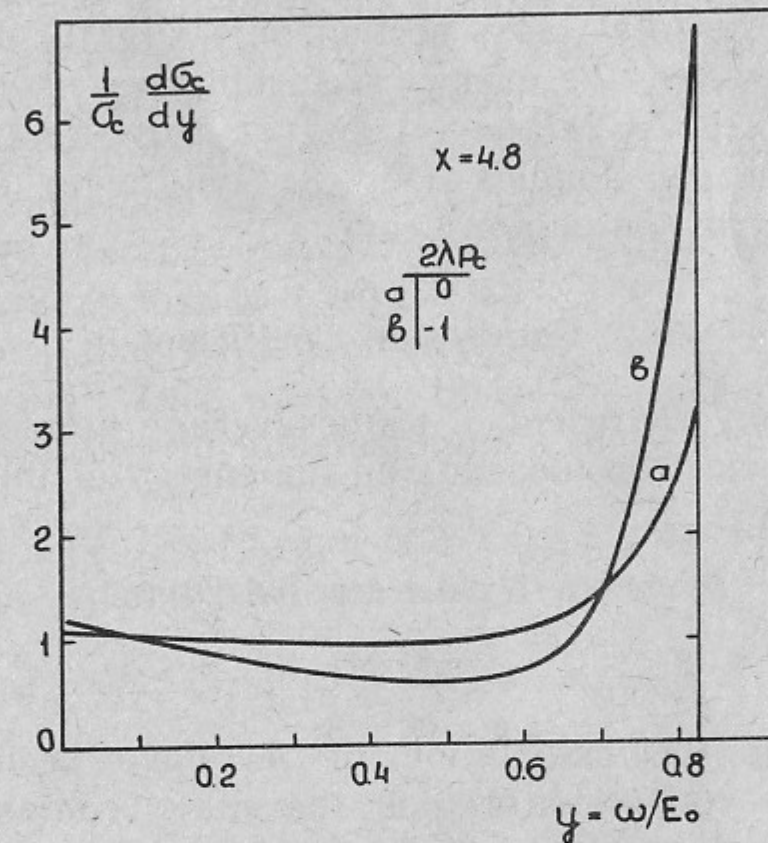


Fig. 3. Energy spectrum of scattered photons.

The energy spectrum of the scattered photons is defined by the cross section (see Fig. 3)

$$\frac{1}{\sigma_c} \frac{d\sigma_c}{dy} \equiv f(x, y) = \frac{2\sigma_0}{x\sigma_c} \left[ \frac{1}{1-y} + 1 - y - 4r(1-r) + 2\lambda P_c r x (1-2r)(2-y) \right],$$

$$y = \frac{\omega}{E_0} \leq y_m = \frac{x}{x+1}, \quad r = \frac{y}{x(1-y)} \leq 1, \quad (5.2)$$

$$\sigma_0 = \pi \left( \frac{e^2}{mc^2} \right)^2 = 2.5 \cdot 10^{-25} \text{ cm}^2.$$

For the polarized beams the spectrum only varies if both electron mean helicity ( $\lambda$ ) and that of the laser photons ( $P_c$ ) are nonzero. The total Compton cross section is

$$\sigma_c = \sigma_c^{np} + 2\lambda P_c \sigma_1,$$

$$\sigma_c^{np} = \frac{2\sigma_0}{x} \left[ \left(1 - \frac{4}{x} - \frac{8}{x^2}\right) \ln(x+1) + \frac{1}{2} + \frac{8}{x} - \frac{1}{2(x+1)^2} \right], \quad (5.3)$$

$$\sigma_1 = \frac{2\sigma_0}{x} \left[ \left(1 + \frac{2}{x}\right) \ln(x+1) - \frac{5}{2} + \frac{1}{x+1} - \frac{1}{2(x+1)^2} \right].$$

In the region of our interest  $x=1 \div 10$   $|\sigma_1/\sigma_c| < 0.2$  and  $\sigma_1=0$  at  $x=2.5$ , i. e. the total cross section only slightly depends on the polarization. However, the energy spectrum does essentially depend on the value of  $\lambda P_c$ . At  $2\lambda P_c = -1$  and  $x > 2$  the relative number of hard photons nearly doubles (Fig. 3) improving essentially the monochromaticity of the photon beam.

## 5.2. Conversion Coefficient

The conversion coefficient, i. e. the average number of scattered photons per one electron, depends on the energy of the laser flash  $A$  and is defined by

$$k = N_\gamma/N \approx 1 - \exp(-A/A_0),$$

$$\sim A/A_0 \quad \text{at } A < A_0. \quad (5.4)$$

Formulae for the calculation of  $A_0$  have been obtained in Ref. [7]. At the conversion region the r.m.s. radius of the laser beam depends on the distance  $z$  to the focus (along the beam) in the following way:

$$r_\gamma = a_\gamma \sqrt{1 + \frac{z^2}{\beta_\gamma^2}}, \quad (5.5)$$

where  $\beta_\gamma = 2\pi a_\gamma^2/\lambda$ ,  $a_\gamma$  is the r.m.s. focal spot radius,  $\lambda$  is the laser wave length. Expression for  $\beta_\gamma$  is valid for a Gaussian shape of the beam in the diffraction limit of focussing. The laser bunch of the length  $l_\gamma$  ( $\sim 2\sigma_\gamma^z$ ) collides at some distance  $b$  from the interaction region with the electron beam of length  $l_e$  ( $\sim 2\sigma_e^z$ ). The radius of the electron beam at the conversion region is assumed to be  $r_e \ll a_\gamma$ . For the case, when  $l_\gamma \approx l_e \gg 2\beta_\gamma$ , the following expression for  $A_0$  can be obtained [7]

$$A_0 \approx \frac{\sqrt{\pi}}{2} \frac{l_e \hbar c}{\sigma_c} = 11 \frac{\sigma_0}{\sigma_c} l_e \text{ (cm), J.} \quad (5.6)$$

The value of  $A_0$  varies only slightly with growth of  $a_\gamma$  until  $2\beta_\gamma < l_e$ , i. e. up to

$$a_\gamma < \sqrt{\lambda l_e / 4\pi}. \quad (5.7)$$

It is reasonable to work at the largest  $a_\gamma$ , given by this formula, since 1) there are fewer problems with hitting the electron beam and 2) the high density of photons is spread over larger region, which is important for reducing nonlinear effects (see Sect. 5.4). The origin of the formulae (5.6), (5.7) can be explained as follows. The probability of an electron collision with the photons of a laser target  $p \sim n_\gamma \sigma_c l$ , where the density of the laser photons at the focus  $n_\gamma \sim A/\pi a_\gamma^2 l \omega_0$ , and the length of the conversion region with high photon density  $l = 2\beta_\gamma = 4\pi a_\gamma^2/\lambda$ . Taking  $l_\gamma = l_e$  we get  $p \sim 1$  at  $A \approx A_0 = \pi \hbar c l_e / 2\sigma_c$ , close to (5.6).

Let us note, that with decreasing of  $a_\gamma$  the conversion length decreases as well. This was not taken into account in the recent paper [41], resulting in underestimation of  $A_0$  by several orders of magnitude.

For  $E_0 = 1$  TeV,  $l_e = 1.5$  mm and  $x = 4.8$  (the advantages of such a value of  $x$  is explained below) we get  $\sigma_c/\sigma_0 = 0.75$ ,  $\lambda = 4 \mu\text{m}$  and

$$A_0 \sim 2.5 \text{ J,}$$

$$a_\gamma < 20 \mu\text{m,} \quad (5.8)$$

$$l_\gamma \sim 1.5 \text{ mm.}$$

At such a focussing the angular divergence of the laser light

$$\alpha_\gamma = a_\gamma/\beta_\gamma = \lambda/2\pi a_\gamma = \sqrt{\lambda/\pi l_e}. \quad (5.9)$$

Formula (5.6) was obtained under the assumption of a head-on collision ( $\alpha_0 = 0$ ). The value of  $A_0$  only slightly varies while  $\alpha_0 < \alpha_\gamma$ . Head-on collisions could be realized using mirrors with holes for electron beams. If the focusing system is outside the beams and  $\alpha_0 \gg \alpha_\gamma$ , then  $A_0$  grows by a factor [7]

$$\chi = \sqrt{\pi} \alpha_0/\alpha_\gamma. \quad (5.10)$$

For example, if  $\alpha_0/\alpha_\gamma = 2.5$  (lenses are outside the beam), then  $\chi = 4$ , and, hence,  $A_0 \sim 10$  J.

### 5.3. Choice of a Laser Wave Length

With increasing energy of laser photons the maximum energy of scattered photons increases also and the monochromaticity improves (for keeping  $k = \text{const}$   $A$  must grow as  $1/\sigma_c(x)$ ). However, besides Compton scattering in the conversion region other processes become possible [7]:

1.  $e + \gamma_0 \rightarrow e + e^+e^-$ ,
2.  $\gamma_0 + \gamma \rightarrow e^+e^-$ .

$$(5.11)$$

In the first process (by Bethe—Heitler) the  $e^+e^-$ -pair is created in the collision of an electron with a laser photon [26], [32]. The threshold of this reaction correspond to  $x=8$  [7]. The cross section (not close to the threshold)

$$\sigma_{\gamma e \rightarrow ee^+e^-} = \frac{28}{9\pi} \alpha \sigma_0 \left( \ln x - \frac{109}{42} \right). \quad (5.12)$$

At  $x < 20$  it is less than that of Compton scattering by two orders of magnitude.

In the second process  $e^+e^-$ -pair is created in a collision of the laser photon with a high energy (scattered) photon. The threshold of this reaction follows from the condition  $\omega_m \omega_0 > mc^2$ , i. e.  $x > 2(1 + \sqrt{2}) \approx 4.8$ . The wave length at  $x=4.8$  is

$$\lambda = 4.2 E_0 (\text{TeV}), \mu\text{m}. \quad (5.13)$$

This region of a wave length is not best for existing lasers, therefore, let us consider what happens at  $x > 4.8$ , i. e. at shorter  $\lambda$ .

The total cross section of the process  $\gamma\gamma \rightarrow e^+e^-$  is [22]

$$\sigma_{\gamma\gamma \rightarrow e^+e^-} = \frac{4\sigma_0}{x_\gamma} \left[ 2 \left( 1 + \frac{4}{x_\gamma} - \frac{8}{x_\gamma^2} \right) \ln \frac{\sqrt{x_\gamma} + \sqrt{x_\gamma - 4}}{2} - \left( 1 + \frac{4}{x_\gamma} \right) \sqrt{1 - \frac{4}{x_\gamma}} \right]; \quad (5.14)$$

where  $x_\gamma = 4 \frac{\omega \omega_0}{m^2 c^4}$  and  $x_\gamma = \frac{x^2}{x+1}$  at  $\omega = \omega_m$ .

In Fig. 4 (curve a) the ratio  $\sigma_{\gamma\gamma \rightarrow e^+e^-} / \sigma_c$  is shown as a function of  $x$ . Above the threshold region the two photon cross section exceeds the Compton one by a factor 1.5—2. The question arises,

what maximum conversion coefficient is possible to obtain, taking into account the loss of photons due to pair creation?

Let electrons traverse the conversion region, where the Compton collision length is  $\lambda_c$ , the pair creation length is  $\lambda_\gamma$  ( $= \text{const}$ , as far as mainly the photons with  $\omega \sim \omega_m$  give contribution to the luminosity).

The kinetic equation has the form:

$$dN_\gamma = N_0 e^{-z/\lambda_c} \frac{dz}{\lambda_c} - N_\gamma \frac{dz}{\lambda_\gamma}, \quad (5.15)$$

where  $N_0$  is the initial number of electrons. The solution of this equation is

$$N_\gamma = N_0 \frac{\lambda_\gamma}{\lambda_c - \lambda_\gamma} (e^{-z/\lambda_c} - e^{-z/\lambda_\gamma}). \quad (5.16)$$

At small  $k$  the relative diminution of the conversion coefficient due to pair creation is:

$$\frac{\Delta k}{k} = \frac{\Delta N_\gamma}{N_\gamma} = -\frac{z}{2\lambda_\gamma} \approx \frac{k}{2} \frac{\lambda_c}{\lambda_\gamma}. \quad (5.17)$$

The maximum number of photons is

$$k_{\max} = \frac{N_{\gamma \max}}{N_0} = \frac{1}{p-1} (p^{1/(1-p)} - p^{p/(1-p)}), \quad (5.18)$$

where  $p = \lambda_c / \lambda_\gamma$ . In Fig. 4 (curve b) is shown the value of  $k_{\max}$  as a function of  $x$ . At large  $x$  the maximum conversion coefficient is 25—30%.

The relationship between conversion coefficients with ( $k$ ) and without ( $k_0$ ) pair creation for  $x=10$  is shown in Fig. 5. One can see that at  $k_0 < 0.3$  the difference between  $k$  and  $k_0$  is small.

At  $x > 4.8$  one should provide removal from the detector not only for  $e^-$  but for  $e^+$  as well. The minimum energy of particles in a pair

$$\varepsilon_{\min} = \frac{m^2}{2\omega_0(1 + \sqrt{1 - 4/x_\gamma})} = \frac{130}{\omega_0(\text{eV})(1 + \sqrt{1 - 4/x_\gamma})} \text{ GeV}. \quad (5.19)$$

So, at  $E_0 = 1$  TeV,  $x=10$  we have  $\omega_0 = 0.62$  eV,  $x_\gamma = 9.9$  and, hence,  $\varepsilon_{\min} = 118$  GeV, i. e. rather high. However, due to repeated collisions  $\varepsilon_{\min}$  will be less by one order of magnitude (see Sect. 8.3).

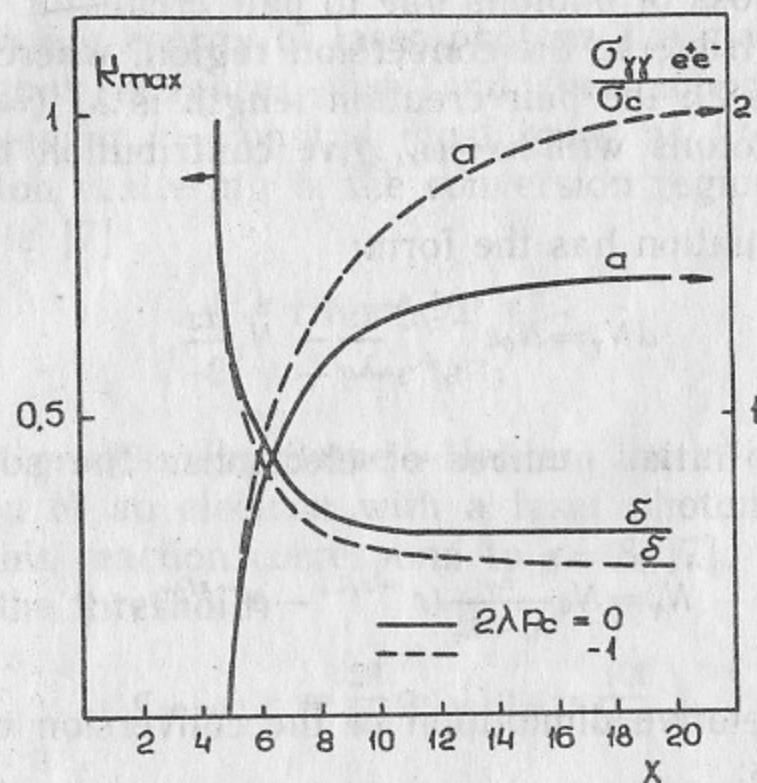


Fig. 4. Curve *a*—dependence of the ratio  $\sigma_{\gamma\gamma \rightarrow e^+e^-}/\sigma_c$  on  $x$ ; *b*—dependence of the maximum conversion coefficient on  $x$ . It is assumed, that  $\omega \approx \omega_m$ .

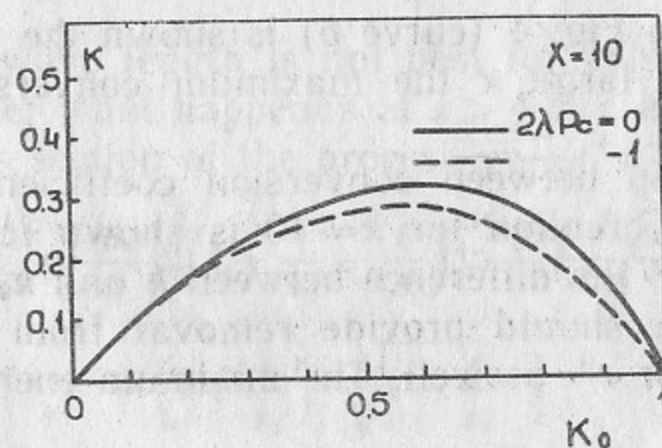


Fig. 5. Connection of the conversion coefficient without ( $k_0$ ) and with ( $k$ ) taking into account pair creation.

With the growth of  $A$  above  $A_0$ , the conversion coefficient increases slower than linearly (eq. (5.4)). Also, repeated scatterings lead to softening of the electron spectrum (bad for beam removal). For these reasons it is better to work at  $k < 0.65$  (or  $A < A_0$ ).

General resume is following: at  $x < 4.8$  one can have  $k \sim 0.65$ , at  $x > 4.8$ —only  $k \sim 0.25$ . As it will be shown in Sect. 7 the ultimate luminosity is restricted by collision effects and  $L_{\gamma\gamma} \propto k^2/(1-k)$ , so that luminosities for  $k=0.25$  and  $k=0.65$  differ by a factor 15.

#### 5.4. Influence of a Strong Field on the Compton Effect

In the conversion region the density of laser photons can be so high, that multiphoton processes occur [24–26]. Nonlinear effects are described in part by the parameter  $\xi$ —the energy acquired by an electron within Compton wave length divided by the photon energy.  $\xi$  is defined by:

$$\xi = \frac{eF\hbar}{m\omega_0c}, \quad (5.20)$$

$F$  is the field strength ( $E, B$ ),  $\omega_0$ —photon energy. At  $\xi \ll 1$  an electron interacts with one photon from the field, but at  $\xi \gg 1$  an electron feels a collective field. For an electron traversing the electromagnetic wave the Compton scattering occurs at  $\xi \ll 1$  or the usual synchrotron radiation may occur at  $\xi \gg 1$  [26]. Similarly, only at  $\xi \ll 1$  is the formula (5.14) for pair creation valid. As soon as spectrum of scattered photons in Compton process is harder than that of synchrotron radiation, we have to work in the region  $\xi \ll 1$ . Let us estimate the value of  $\xi$  at  $k \sim 1$ .

The field in the laser focus is

$$F^2 \approx \frac{4A}{a_\gamma^2 c \tau}, \quad (5.21)$$

where  $A$ —the flash energy, and  $\tau$  is the duration. From here

$$\xi^2 = A/\bar{A}; \quad \bar{A} = \frac{c\tau}{4} \left( \frac{m\omega_0 a_\gamma c}{e\hbar} \right)^2. \quad (5.22)$$

Substituting from (5.6), (5.7)  $a_\gamma \sim \sqrt{\lambda l_e/4\pi}$ ,  $A \approx kA_0 \approx k\hbar c l_e/\sigma_c$ ,  $c\tau \approx l_e$ , we get

$$\xi^2 = \frac{4}{\alpha\pi^2} \frac{\sigma_0}{\sigma_c} \frac{\lambda}{l_e} k, \quad (5.23)$$

where according (5.1),  $\lambda \approx 20 E_0(\text{TeV})/x$ ,  $\mu\text{m}$ . For VLEPP with  $l_e = 0.15$  cm at  $x = 4.8$  and  $k = 0.5$ , we have

$$\xi^2 \approx 0.1 E_0 (\text{TeV}). \quad (5.24)$$

Such a value of  $\xi$  may be considered as acceptable, but at the limit. It is seen, that with increasing  $E_0$  or decreasing  $l_e$ , one can get  $\xi > 1$ . It does not mean, that it is not possible to work with such accelerator parameters. Formula (5.2) was obtained under assumption that the length of the conversion length  $\sim l_e$  (then we get a minimum  $A_0 \propto l_e$ ). By increasing the conversion length and flash duration ( $l_\gamma \sim 2\beta_\gamma \gg l_e$ ) one can again get  $\xi \ll 1$ . Then in the formulae for  $A_0$  and  $\xi^2$ ,  $l_e$  should be replaced by  $l_\gamma$ .

### 5.5. Lasers

Let us summarize once again the essential requirements for laser parameters to provide  $k \sim 0.65$  at  $x = 4.8$ .

Flash energy	$A \sim 2.5$ J	
Repetition rate	$f = 100$ Hz (for the VLEPP)	
Duration	$c\tau \sim 1.5$ mm	(5.25)
Wave length	$\lambda \sim 4.2 E_0 (\text{TeV}), \mu\text{m}$	
Angular divergence	near to diffraction limit	

Now we can give some general considerations about the choice of a possible laser.

**Solid state** lasers have flash energies considerably higher, than is necessary for our purpose, but at a low repetition rate. With a specially developed laser it should be possible to get simultaneously the all required parameters  $A$ ,  $f$ ,  $\tau$ . However, solid state lasers have, as a rule, a wave length less than  $1 \mu\text{m}$  ( $\lambda = 1.06 \mu\text{m}$  — neodymium glass), i. e. for  $E_0 = 1$  TeV we will have  $x \sim 20$ . Hence, pair production is possible and, therefore,  $k < 0.25$  (see Sect. 5.3). Another problem is obtaining short bunches with diffraction divergence and synchronization with the electron beam.

**Gas lasers** can work from ultra-violet (eximers) up to  $\lambda = 5 - 10 \mu\text{m}$  ( $\text{CO}, \text{CO}_2$ ) with fewer problems with repetition rate and divergence, than with solid state lasers. In other respects the problems are approximately the same.

**Free-electron lasers.** In Ref. [9] it was suggested to use for this purpose a one-pass free electron laser (FEL). In their scheme the

photon bunch with  $\lambda \sim 1 \mu\text{m}$  is generated by the main electron beam when its energy is 10 GeV. It seems more rational to use a separate linac for FEL, so that there is no need to transport the light bunch along a 10 km length.

It is of interest, that for a 5 TeV collider a wave length of  $20 \mu\text{m}$  is needed. If an electron bunch of such a length is prepared, it will generate light in the undulator coherently without any pre-bunching.

Another FEL scheme is also possible with the storage of the light between mirrors at storage ring of a few hundreds MeV energy.

For our purpose FELs have evident advantages: tunable wave length, adequate repetition rate and duration, and simplicity of synchronization. Unfortunately, the world experience in this field is limited.

## 6. SCHEME OF $\gamma\gamma$ -, $\gamma e$ -COLLISIONS

### 6.1. General Scheme of the Interaction Region

After conversion at a distance  $b$  from the interaction point (i.p.) electrons and photons travel in the direction of the i.p. Without preventive measures, soft electrons will scatter on the opposing beam, with a large angular spread. Moreover, in the strong fields various collision effects will take place (see Sect. 7), restricting  $\gamma\gamma$ - and  $\gamma e$ -luminosities.

More attractive is the following scheme for an interaction region (Fig. 6). After conversion, the electrons with a wide energy spectrum cross a region with a transverse magnetic field  $B_e$ , where they are deflected in the horizontal direction ( $x$ ). Passing by each other, beams are repulsed in the same plane (if the deflection is much larger than the vertical beam size). As a result, the beam keeps a small vertical angular divergence and can be removed through a narrow horizontal slit in the lenses. Besides, due to predeflection by the external field, soft particles scatter on the opposing beam at relatively small angles. This circumstance is of great importance in the scheme, where beams collide at some crossing angle. Removal of particles is considered in detail in Sect. 8.

## 6.2. Problems

In the scheme of  $\gamma\gamma$  or  $\gamma e$  colliding beams the following problems of principal and also of a technical character are seen:

1. There are collision effects restricting the luminosity. The most serious restrictions arise for  $\gamma e$ -collisions.

2. A difficult problem is the removal of «used» electrons after conversion. These electrons have energies in the range  $E = (0.02 \div 1)E_0$  (see Sect. 8.3). They should be removed from the detector without losses on lenses and other elements. One absorbed electron of TeV energy creates about 200 neutrons. From here the requirements are seen. The task is complicated by deflection of particles in the field of the opposing beam.

3. The power of all photons is comparable with that of the electron beam. They also have to be removed outside the detector and accelerator.

4. Electromagnetic focusing lenses and bending magnets should not be placed in the pass of laser light.

5, 6. Last, for obtaining the high luminosity, the  $e^+e^-$ -collider itself and the laser with the required parameters must be built.

## 7. BEAM COLLISION EFFECTS

In the interaction region electrons and photons are influenced by the field of the opposing beam. In the case of  $\gamma\gamma$ -collisions the field is created only by electrons, deflected after conversion by the external field. In  $\gamma e$ -collisions the field is created also by main electron beam used for  $\gamma e$ -collisions. The strong field leads to increased energy spread of the electrons (in  $\gamma e$ -collisions) and also to conversion of photons into  $e^+e^-$ -pairs (in  $\gamma\gamma$ - and  $\gamma e$ -collisions). A resolution of these problem is connected inevitably with a loss of luminosity. Below we will consider these and other collision effects.

### 7.1. Coherent Pair Creation in the Beam Field

In a strong transverse magnetic (electric) field created by the opposing beam a photon have probability of conversion into  $e^+e^-$ -pair [33—36]. The importance of this process for linear colliders was pointed out in Ref. [37, 38].

The probability of pair creation per unit length by a photon with the energy  $\omega$  in the magnetic field  $B$  ( $|B| + |E|$  for our case) is [34]

$$\mu(\kappa) = \frac{\alpha^2 B}{r_e B_0} T(\kappa), \quad (7.1)$$

where

$$\kappa = \frac{\omega}{mc^2} \frac{B}{B_0}, \quad B_0 = \frac{m^2 c^3}{eh} = 4.4 \cdot 10^{13} \text{ Gs},$$

$$T(\kappa) \approx 0.16 \kappa^{-1} K_{1/3}^2(4/3\kappa). \quad (7.2)$$

A plot of the function  $T(\kappa)$  is shown in Fig. 7. In the asymptotical limits

$$T(\kappa) = 0.23 \exp(-8/3\kappa), \quad \kappa \ll 1,$$

$$T(\kappa) = 0.38 \kappa^{-1/3}, \quad \kappa \gg 1. \quad (7.3)$$

In the our case  $\omega \sim E_0$ , therefore one can puts  $\kappa \sim \Upsilon = \gamma B/B_0$ , and then

$$\mu(\Upsilon) \approx \frac{\alpha^2 \Upsilon}{r_e \gamma} T(\Upsilon). \quad (7.4)$$

Intensive pair production begins at  $\Upsilon > 1$ . This can be seen from the following arguments. In the frame of the pair c.m. at  $\Upsilon \sim 1$  the electron acquires within one Compton wave length an energy equal to its rest mass.

Let us obtain an expression for  $\Upsilon$ . After conversion, the electrons are swept aside by the magnetic field  $B_e$  and pass the i. p. at some distance  $x_0$  ( for  $E = E_0$ , Fig. 6). The field at the i. p. is produced mostly by particles which have not lost energy in the conversion region, since they pass closer to the i.p. Their field is

$$|E| + |B| = 2eN(1-k)/\sigma_z x_0,$$

From here

$$\Upsilon_1 \approx \frac{2N(1-k)r_e^2 \Upsilon}{\alpha \sigma_z x_0}. \quad (7.5)$$

In  $\gamma e$ -collisions photons are influenced also by the opposing electron beam, moving along the axis. Inside a flat beam ( $\sigma_x \gg \sigma_y$ )

$$\bar{\Upsilon}_0 \sim \frac{Nr_e^2 \Upsilon}{\alpha \sigma_x \sigma_z}. \quad (7.6)$$

Further we will provide  $\Upsilon$  with the index 0 or 1 for designation of field source: 0—not deflected beam (sometimes we will call it as

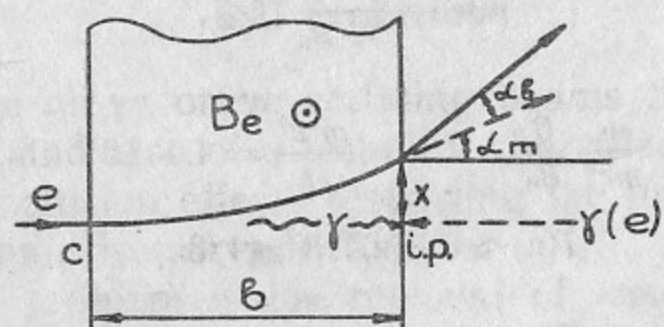


Fig. 6. Scheme of interaction region and removal of electrons.

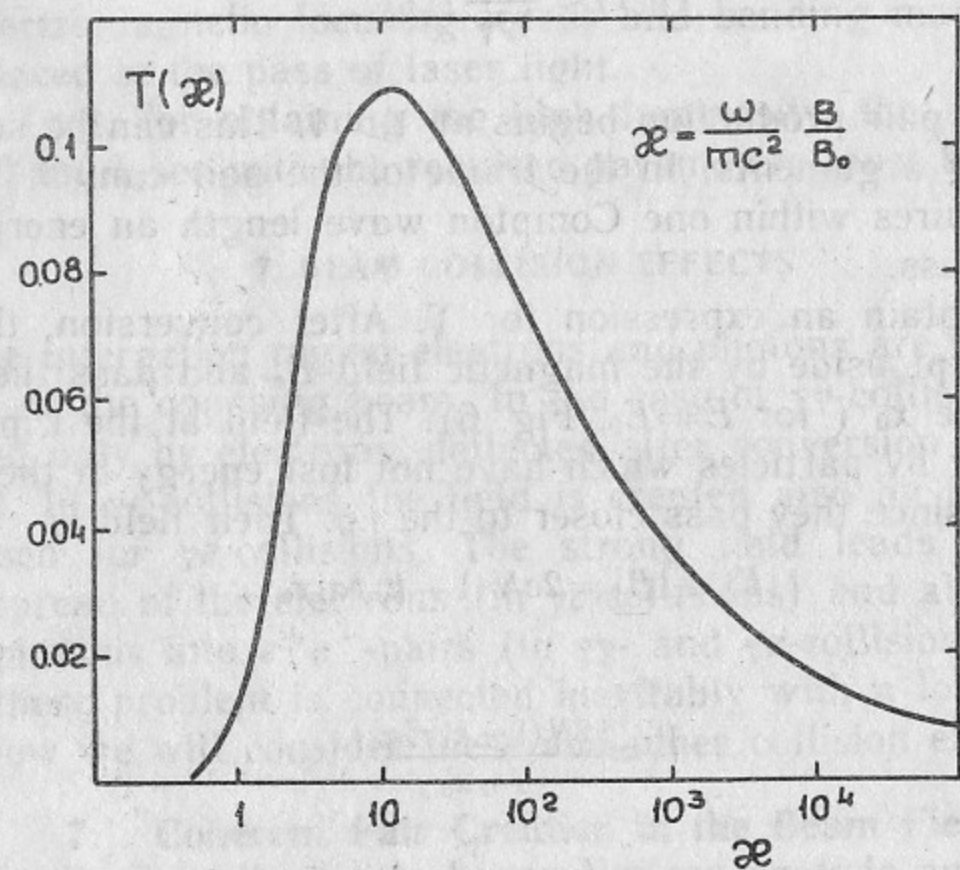


Fig. 7. Function  $T(x)$  in the formula (7.1).

«main electron beam»), 1 — for the beam, deflected after conversion.

Let us determine the minimum energy of the produced particles. At the threshold of the reaction ( $\Upsilon < 1$ ) the energy of particles of the pair  $\sim \omega/2$ . At  $\Upsilon \gg 1$  an estimation can be done as follows. In the c.m. system of the pair we find, that the invariant mass of the pair is about  $W \approx 2\gamma'eB\lambda_c$ , where  $B\gamma'$  is electric field in this system, and  $\gamma' = \omega/W$ . From here  $W^2 \approx 2eB\omega\lambda_c$ . In the decay of this system into  $e^+e^-$ -pairs along the direction of motion the minimum energy will be (at  $W \gg mc^2$ )

$$\varepsilon_{\min} \approx \frac{\omega m^2}{W^2} = \frac{m}{2} \frac{B_0}{B} = \frac{E_0}{2\Upsilon_0}. \quad (7.7)$$

Though this is very rough estimate, it is in agreement with the exact formula for the spectrum [36, 38]. At  $\Upsilon \gg 1$  ( $\kappa = \Upsilon$  in our case) the spectrum has a saddle like shape with enhancements at the edges at  $\varepsilon/\omega = 1.6/\Upsilon$  and  $1 - 1.6/\Upsilon$ . In the region  $\varepsilon < 0.5E_0/\Upsilon$  the spectrum has the exponential fall off. For further estimations we put the minimum energy to be  $\varepsilon_{\min} = 0.2E_0/\Upsilon$ . Below this bound the number of particles is negligible.

The probability to create a pair during the time of collision is:

$$\rho \approx \mu \sigma_z = \frac{\alpha^2 \sigma_z}{r_e \gamma} \Upsilon T(\Upsilon). \quad (7.8)$$

From here, at a given probability of pair creation  $\rho$  one can find  $\Upsilon$ , which is a function of one variable:

$$\rho_1 = \rho \frac{r_e \gamma}{\alpha^2 \sigma_z}. \quad (7.9)$$

With a sufficient accuracy (better than 25%) the solution of (7.8) can be approximated as

$$\Upsilon = \begin{cases} 2.7/\ln(0.1/\rho_1), & \rho_1 < 0.01 \\ 1.2 + 9 \cdot \rho_1, & 0.01 > \rho_1 < 4 \\ 4.5 \cdot \rho_1^{3/2}, & \rho_1 > 4 \end{cases} \quad (7.10a)$$

$$1.2 + 9 \cdot \rho_1, \quad 0.01 > \rho_1 < 4 \quad (7.10b)$$

$$4.5 \cdot \rho_1^{3/2}, \quad \rho_1 > 4 \quad (7.10c)$$

For clarification of qualitative dependence it is useful to simplify these expressions

$$\Upsilon = \begin{cases} 1, & 0.001 < \rho_1 < 0.1 \\ 10 \cdot \rho_1, & 0.1 > \rho_1 < 5 \\ 4.5 \cdot \rho_1^{3/2}, & \rho_1 > 5 \end{cases} \quad (7.11a)$$

$$10 \cdot \rho_1, \quad 0.1 > \rho_1 < 5 \quad (7.11b)$$

$$4.5 \cdot \rho_1^{3/2}, \quad \rho_1 > 5 \quad (7.11c)$$

The accuracy of approximation (7.11) is about 2 at  $p_1 < 0.25$  and better than 25% for larger  $p_1$ . In the case b) it is assumed in fact, that  $T=0.1$  in the range  $Y=1 \div 50$ . The characteristic values of  $p_1$  are:  $p_1=0.14 \cdot p$  for VLEPP and  $p_1=0.75 \cdot p$  for TLC. At multi-TeV colliders one expect to use shorter bunches, so that  $p_1$  can be considerably larger.

## 7.2. Restriction on a Luminosity in $\gamma\gamma$ -Collisions due to Coherent Pair Creation

Pair creation in the field of the deflected beam is determined by the parameter  $Y_1$ . From  $Y_1$  one can obtain the required separation at i.p.

$$x_0 = \frac{2N(1-k) \gamma r_e^2}{\alpha \sigma_z Y_1} \quad (7.12)$$

To provide the deviation  $x_0$  in the field  $B_e$  it is necessary to have a distance between the conversion region and i.p.

$$b^2 = \frac{2E_0 x_0}{eB_e} = \frac{4N(1-k) r_e^3 \gamma^2 B_0}{\alpha^2 \sigma_z Y_1 B_e} \quad (7.13)$$

Let us assume that the emittance of electron beams is very small and the transverse size of the photon beam at the i.p. is determined by Compton scattering, i. e.  $a_\gamma \sim b/\gamma$ . Then the  $\gamma\gamma$ -luminosity

$$L_{\gamma\gamma} \approx \frac{N^2 f k^2 (1-p)}{4\pi a_\gamma^2} \sim \frac{N f \alpha^2 k^2 (1-p) \sigma_z B_e}{16\pi (1-k) r_e^3 B_0} Y_1 \quad (7.14)$$

The omitted numerical coefficient is 0.85 for polarized ( $2P_c \lambda = -1$ ) and 0.4 for nonpolarized beams. The factor  $(1-p) \sim (1-0.5p)^2$  at small  $p$  means diminution of the number of photons due to conversion into  $e^+e^-$ -pairs. Substituting  $Y_1$  from (7.11) we get the  $\gamma\gamma$ -luminosity for three regions of  $p_1$ :

$$\frac{N f \alpha^2 k^2 \sigma_z B_e (1-p)}{16\pi (1-k) r_e^3 B_0}, \quad (7.15a)$$

$$L_{\gamma\gamma} \approx \frac{N f \gamma k^2 B_e p (1-p)}{1.6\pi r_e^2 B_0 (1-k)}, \quad (7.15b)$$

$$\frac{N f B_e}{4\pi \alpha r_e^2 B_0} \left( \frac{\gamma^3 r_e p}{\sigma_z} \right)^{1/2} \frac{k^2 (1-p)}{1-k}. \quad (7.15c)$$

We see, that working in the regime (a), when the pair creation probability is small, the luminosity  $L_{\gamma\gamma} \propto \sigma_z$  and does not depend on the beam energy. With the growth of  $p_1$  the dependence of  $L_{\gamma\gamma}$  on  $\sigma_z$  changes: in the regime (b), it does not depend on  $\sigma_z$ ; in (c), it even increases with decreasing  $\sigma_z$ . Also in the region (b) and (c)  $L_{\gamma\gamma}$  grows with increasing beam energy.

It follows from eq. (7.14) that  $L_{\gamma\gamma} \propto Y_1$ , i. e. the larger pair creation probability we allow, the larger luminosity we can obtain. The regime of low  $p$  corresponds to  $Y_1 \ll 1$ . What restrictions exist on the value of  $p$ ? Formally, the luminosity grows up to  $p \sim 0.5$ . However, there are two effects, not studied yet, which can restrict  $p$  at a much lower level.

1. Electrons and positrons produced by the photon are separated by the field of the opposing deflected beam. These separated particles produce their own field in the region of the photon beam (on axis), that can increase the pair creation probability. This field affects also the motion of  $e^-$  and  $e^+$  themselves. So a rather complicated picture emerges.

Let us consider the field acting on a photon travelling from left to right. The particles, moving in the same direction, do not influence it (electrical and magnetic forces are opposite). One has take into account only the field of opposing swept electrons and separated  $e^+$  and  $e^-$ . These fields are added or subtracted depending on the types of primary particles and the direction of bending. Fig. 8 shows various combinations. The fields are added in the cases *a* and *d*, but subtracted in *b* and *c*. In the latter cases some sort of field screening on axis can occur, which is very useful. Good cases from this respect have also some disadvantages. So, in *b* the swept beams scatter on each other not only in the plane of the picture, but in a vertical direction as well, causing an additional background. In the case *c* positron beams are required.



2. Second effect. Let us assume for a moment that the  $e^+e^-$ -particles are not separated by the field of the opposing deflected beam. Nevertheless, in the collision of neutral beams, consisting

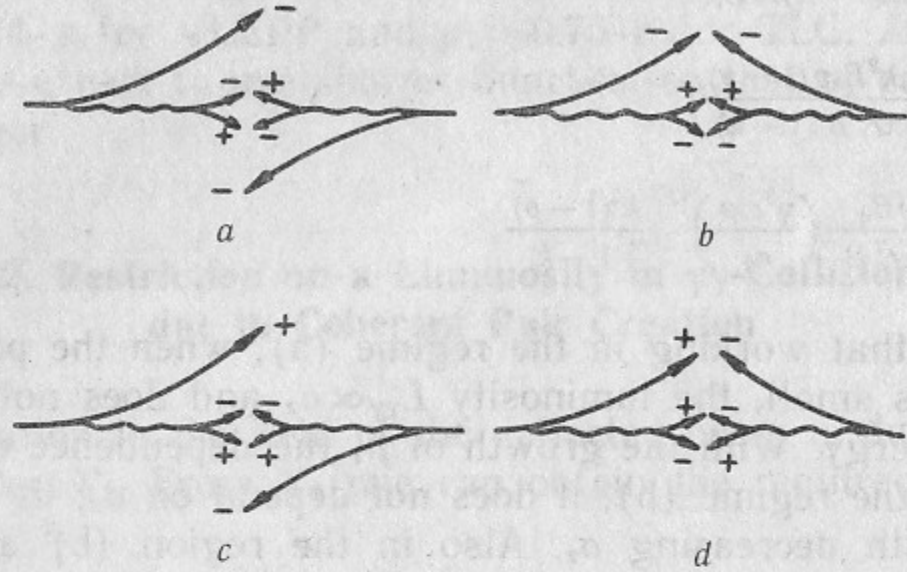


Fig. 8. Field sources at the interaction region.

of  $e^+e^-$ -pairs, at certain conditions an instability can occur [14]. The criteria of the instability is approximately the same as for charged beams (eq. (2.11)).

These questions need further detailed consideration. Arising fields influence also the deflection angles, which determine the removal scheme.

At small  $p$  all these effects are not essential. For colliders of TeV energy the luminosity depends only slightly on  $p_1$  (see eq. (7.10)), therefore, in the following, we will consider here only this case. Let assume for estimation  $\Upsilon_1=1$ . Then

$$L_{\gamma\gamma} \approx \frac{Nf\alpha^2 k^2 \sigma_z B_e}{16\pi(1-k)r_e^2 B_0} \quad (7.16)$$

For  $k=0.5$ ,  $B_e=30$  kGs, we get

$$L_{\gamma\gamma} \approx 1.6(N/10^{10}) f \text{ (Hz)} \cdot \sigma_z \text{ (cm)} \cdot 10^{32}, \text{ cm}^{-2}\text{s}^{-1}. \quad (7.17)$$

Hence

$$\begin{aligned} \text{for VLEPP} \quad L_{\gamma\gamma} &\sim 2.5 \cdot 10^{34} \text{ cm}^{-2}\text{s}^{-1}. \\ \text{for TLC} \quad L_{\gamma\gamma} &\sim 5.5 \cdot 10^{33} \text{ cm}^{-2}\text{s}^{-1}. \end{aligned}$$

At  $k=0.65$  the luminosity will be larger by additional factor 2.4.

We see, that the restriction on the  $L_{\gamma\gamma}$  luminosity due to coherent pair creation occurs at a rather high level, even higher than the luminosity attainable in  $e^+e^-$ -collisions.

### 7.3. Restriction on $L_{\gamma e}$ due to Coherent Pair Creation

In the case of  $\gamma e$ -collisions the photons are affected mainly by the field of the opposing electron beam. The corresponding parameter is  $\Upsilon_0$  (eq. (7.6)). The dependence of  $\Upsilon_0$  on beam parameters and the probability of pair creation is given by the same formula (7.10). At fixed  $N$ ,  $\sigma_z$ ,  $\gamma$  pair creation is controlled by the horizontal beam size  $\sigma_x$ .

Let the beam separation at the i.p. be

$$x_0 = s\sigma_x. \quad (7.18)$$

(The ratio  $s=x_0/\sigma_x$  will be discussed further together with other effects: beam energy losses, displacement etc.)

The distance between the conversion region and the i.p. is found from eq. (7.13) (with replacement of  $\Upsilon_1$  by  $\Upsilon_0$ ). At the i.p. the flat electron beam collides with the photon beam having the vertical size not less than  $b/\gamma$ . The  $\gamma e$ -luminosity will be

$$L_{\gamma e} \sim \frac{N^2 f k \gamma (1-0.5p)}{4\pi b \sigma_x}, \quad (7.19)$$

where

$$\sigma_x = \frac{N r_e^2 \gamma}{\alpha \sigma_z \Upsilon_0}, \quad (7.20)$$

$$b^2 = \frac{2e\gamma\sigma_x s}{r_e B_e}. \quad (7.21)$$

In the result

$$L_{\gamma e} = \frac{\alpha^2 f \sigma_z \Upsilon_0 (1-0.5p) k}{4\pi r_e^3 \gamma} \left( \frac{B_e \sigma_z \Upsilon_0 N}{2B_0 s} \right)^{1/2}. \quad (7.22)$$

For three ranges (7.11) of  $p_1$  values we obtain

$$\frac{0.055 f k \alpha^2 \sigma_z (1-0.5p)}{r_e^3 \gamma} \left( \frac{B_e \sigma_z N}{2B_0 s} \right)^{1/2}, \quad (7.23a)$$

$$L_{\gamma e} = \frac{1.75 f k (1-p) p}{r_e^2} \left( \frac{B_e N p \gamma}{B_0 s} \right)^{1/2}, \quad (7.23b)$$

$$\frac{0.5 f k (1-0.5p)}{\alpha r_e^2} \left( \frac{N \gamma B_e}{B_0 s} \right)^{1/2} \left( \frac{p^3 \gamma r_e}{\alpha^2 \sigma_z} \right)^{3/4}. \quad (7.23c)$$

In these formulae we have not determined yet the values of  $s$  and  $p$ . The two next subsections are devoted to this subject. After considering all effects a summary of physical effects determining  $L_{\gamma e}$  will be made.

#### 7.4. Radiation Energy Losses of Electrons in $\gamma e$ -Collisions

The fields of opposing particles lead to bremsstrahlung radiation of electrons. The relative losses have to be restricted. There are two sources of the field:

1. The electron beam, swept aside after conversion.

2. The  $e^+e^-$ -pairs, created by photons. The field in this case arises in the following way. Under the influence of the main electron bunch the created electrons are bent away from the collision area, so that positrons remain inside the beam and produce the field.

From here arise the main requirements to the beam separation and maximum pair creation probability.

Let us consider the first effect. At the i.p. the field is produced mainly by  $N(1-k)$  unscattered electrons, since they travel closer to the axis. Assuming an uniform density of particles on the length  $2\sigma_z$ , it is easy to get the relative energy losses when an electron passes at the distance  $x_0$  from the deflected beam (comp. (2.8))

$$\delta = \frac{8r_e^2 N^2 \gamma (1-k)^2}{3\sigma_z x_0^2} F_{\gamma_1} = \frac{2\alpha^2 \sigma_z}{3r_e \gamma} \gamma_1 (F_{\gamma_1} \gamma_1), \quad (7.24)$$

where  $\gamma_1$  defined by (7.5). The function  $F_{\gamma_1}=1$  for  $\gamma_1 \ll 1$  and  $(F_{\gamma_1} \gamma_1) \approx \gamma_1 / (5\gamma_1 + 1)$  for  $\gamma_1 < 100$  (my approximation of numerical calculation of Ref. [15]). From here

$$\gamma_1 = 2.5u + \sqrt{6.25u^2 + u}, \quad (7.25)$$

where

$$u = \frac{3\delta r_e \gamma}{2\alpha^2 \sigma_z}$$

From formulae (7.5), (7.6), (7.24) we get the required separation

$$x_0 = \frac{4\alpha r_e N(1-k)}{3\delta} (F_{\gamma_1} \gamma_1) \quad (7.26)$$

and the ratio

$$s = \frac{x_0}{\sigma_x} = \frac{2(1-k)\gamma_0}{\gamma_1}. \quad (7.27)$$

The value of  $\gamma_1$  was determined just above, and the value of  $\gamma_0$  is given by (7.10), (7.11). Let us calculate  $s$  for small pair creation probability, i. e.  $\gamma_0 \sim 1$ . For  $\delta=0.05$  and  $k=0.5$  from (7.25) we get for VLEPP  $u=0.01$ ,  $\gamma_1=0.13$  and  $s \approx 8$ , for TLC  $u=0.055$ ,  $\gamma_1=0.4$  and  $s \approx 2.5$  (this result will be discussed in Sect. 7.6).

In the similar way from (7.27) one can find  $s$  for the arbitrary case, and  $s$  will depend on the pair creation probability. The maximum value of  $p$  (when the luminosity is also maximum) is restricted by the energy losses in the field of created pairs (see beginning of this subsection). In this paper we will not consider in detail a general case of  $\gamma e$ -collisions (and  $\gamma\gamma$  as well), since for colliders of TeV energy  $\gamma$  can not exceed essentially 1 (see eq. (7.10)).

#### 7.5. Spin Rotation

When the electron is bent by the angle  $\theta$ , its spin rotates relative to its trajectory by the angle [26]

$$\theta' = \frac{\mu'}{\mu_0} \gamma \theta = \frac{\alpha \gamma}{2\pi} \theta, \quad (7.28)$$

where  $\mu_0$  and  $\mu'$  are normal and anomalous magnetic moments of the electron. In our case electrons of the main beam are bent during collision through the angle

$$\theta = \frac{2r_e N(1-k)}{\gamma x_0}, \quad (7.29)$$

then

$$\theta' = \frac{\alpha r_e N(1-k)}{\pi x_0}. \quad (7.30)$$

The longitudinal polarization decreases by 5% at  $\theta' < 1/3$ . From here we get the required separation

$$x_0 > \alpha r_e N(1-k). \quad (7.31)$$

This should be compared with the expression (7.26), obtained from the beamstrahlung energy losses. In the case of small  $\gamma_1$  and  $\delta$  the condition (7.31) is more stringent. For VLEPP and TLC at  $E=1$  TeV, however, the condition (7.26) is decisive.

### 7.5.2. Displacement of the Electron Beam

During collision the electron bunch displaces in the field of the opposing deflected beam through the distance

$$\Delta x = \frac{\sigma_z r_e N (1-k)}{\gamma x_0} \quad (7.32)$$

To keep the luminosity unchanged it is necessary to have  $\Delta x < \sigma_x$ . In our case

$$\frac{\Delta x}{\sigma_x} = \frac{\alpha^2 \sigma_z^3 \gamma_0^2 (1-k)}{\gamma^3 N r_e^3 s} \quad (7.33)$$

Analysis of various cases shows, that this ratio is larger for colliders with lower energy and longer bunches. So for VLEPP at  $k=0.5$   $\Delta x/\sigma_x \sim 0.3 \cdot \gamma_0/s E_0$  (TeV). We see, that, if we decrease the energy at  $\gamma_0 \sim 1$  and  $s \sim 5 \div 10$ , then at  $E_0 < 0.3$  TeV we will have  $\Delta x/\sigma_x > 1$ . For  $E_0 \sim 1$  TeV this displacement is little. Let us note, if we would not deflect the beam after conversion at all or do it in the vertical plane, then the displacement should be compared with a considerably smaller vertical beam size. The separation provides also small deflection angles of soft particles in collision with the opposing beam (Sect. 8.3).

### 7.5.3. Angular Spread of Particles in $\gamma e$ -Collisions

At  $\gamma_0 \gg 1$  photons create inside the electron beam  $e^+e^-$ -pairs with a fairly small minimum energy (7.7)  $E \sim 0.2 E_0/\gamma_0$ . The produced electrons are repulsed from the opposing electron bunch and deflect through some angle. Assuming, that the field of a flat beam is  $2B = \pi e N/\sigma_x \sigma_z = \text{const}$  up to distances  $\sim 2\sigma_x$ , and is zero at larger distances, we find the deflection angle for a particle with the energy  $E$

$$\begin{aligned} \theta &\sim \frac{\pi N e^2}{\sigma_x E} & \text{at } \theta < 4\sigma_x/\sigma_z, \\ \theta &\sim \left( \frac{4\pi N e^2}{\sigma_z E} \right)^{1/2} & \text{at } \theta > 4\sigma_x/\sigma_z. \end{aligned} \quad (7.34)$$

The deflection angles in the horizontal and vertical directions are of the same order, as soon as at distances of about  $\sigma_x$  from the axis the field is almost symmetrical.

It is seen, that for large  $\gamma_0$  and short bunches the deflection angles are large, i. e. there will be problems with beam removal.

### 7.6. Estimation of $L_{\gamma e}$

We will restrict ourselves to the case in which coherent pair creation is negligible, i. e.  $\gamma_0 \sim 1$ . As was already explained, this case describe rather well the situation for TeV energy colliders. For general cases essential side effects were pointed out, and are needed in additional studies. For  $\gamma_0 = 1$  the  $\gamma e$ -luminosity is restricted by the value (see eq. (7.22))

$$L_{\gamma e} \approx \frac{\alpha^2 f \sigma_z k}{4\pi r_e^3 \gamma} \left( \frac{B_e \sigma_z N}{2B_0 s} \right)^{1/2} \quad (7.35)$$

In the preceding section we have considered factors determining the required deflection of the electron beam after conversion. At  $E_0 = 1$  TeV all is determined by beamstrahlung energy losses. The separations we obtained are  $s=8$  for VLEPP and 2.5 for TLC. In the latter case some overlapping of  $e^+e^-$ -beams remains. Therefore, let us increase the separation up to  $s \sim 5$ . Assuming in both cases  $s=5$  at  $k=0.5$ ,  $B_e=30$  kGs, we get

$$L_{\gamma e} = \frac{0.7 \cdot 10^{32}}{E_0(\text{TeV})} \sqrt{\frac{N}{10^{10}}} \sigma_z^{3/2} (\text{cm}) f (\text{Hz}), \quad \text{cm}^{-2}\text{s}^{-1}. \quad (7.36)$$

From here, the maximum luminosity of  $\gamma e$ -collisions is for

$$\begin{aligned} \text{VLEPP:} & \quad L_{\gamma e} \sim 6 \cdot 10^{32} \text{ cm}^{-2}\text{s}^{-1}, \\ \text{TLC:} & \quad L_{\gamma e} \sim 3.5 \cdot 10^{32} \text{ cm}^{-2}\text{s}^{-1}. \end{aligned} \quad (7.37)$$

We see, that  $L_{\gamma e}$  is smaller than  $L_{\gamma\gamma}$  (7.17) by about a factor 30. For TeV energies it is desirable to have  $L_{\gamma e}$  at least one order higher.

## 8. REMOVAL OF PHOTONS AND ELECTRONS FROM THE CONVERSION AND INTERACTION REGION

### 8.1. General Remarks

Due to problems in obtaining high luminosity in  $\gamma e$ -collisions, and for brevity, we will consider further only  $\gamma\gamma$ -collisions.

Removal of particles from the interaction region is a difficult task. Something similar takes place in  $e^+e^-$ -collisions at large  $\Upsilon$ .

At last few years a scheme of  $e^+e^-$ -collisions is discussed where beams collide at some crossing angle  $\alpha_c$  with respect to the direction of the beam motion, so that after the collision, the disrupted beams travel outside of the lenses. Usually the luminosity drops, if  $\alpha_c > \sigma_x/\sigma_z$ . This problem can be solved [40] by turning each bunch relative to the average trajectory by the angle  $\alpha_c/2$  with help of RF field, Fig. 9. This type of collisions is called «crab-crossing».

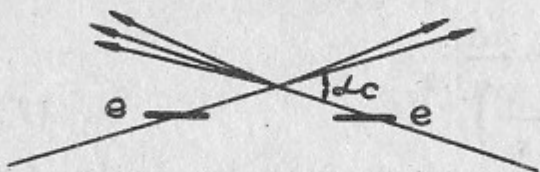


Fig. 9. «Crab-crossing».

It looks like a head-on collision, but all particles have a component of velocity transverse to the collider. Here there is no luminosity loss. Such a method of collisions is, perhaps, unique at  $\Upsilon \gg 1$ , when a lot of soft particles are created (due to beamstrahlung and pair creation), having large disruption angles. A similar approach can be applied to the  $\gamma\gamma$ -collisions. We will consider this scheme as basic.

In principle,  $\gamma\gamma$ -collisions can be arranged with zero crossing angle, since, owing to advanced separation of beams, all the particles travel after the collision within a narrow horizontal plane and they can be removed through a slit in the lenses. In this case one has to use kicker magnets. It is, of course, a difficult task, since the particles after conversion have a wide energy spectrum. The first (basic) scheme looks much more elegant.

## 8.2. Removal of Photons

If the beams collide at a large enough crossing angle (Fig. 9, 10,a), photons travel outside without any problems. There is only one question: how to arrange the crossing angle? This angle can be arranged as an angle between two halves of the collider; or both halves lay on one axis and only the nearby collision region beams are bent by the angle of about ten milliradians (we discuss now the change of direction of motion, but not the turning of the beam relative to the average line). In the first case the crossing angle is fixed permanently, which is not convenient. In the second approach there is also one defect. It is desirable to have a collision of longitudinally polarized beams. At the bending angle  $\varphi$  the spin of the electron turns by the angle (comp. (7.28))

$$\varphi' = \frac{\mu'}{\mu_0} \varphi \gamma \approx \frac{\alpha \gamma}{2\pi} \varphi. \quad (8.1)$$

So at  $\varphi = \alpha_c/2 = 5$  mrad  $\varphi' = 3.6 \cdot E_0$  (TeV), i. e. the spin angle depends essentially on the beam energy. In principle, one can make compensation before injection to the collider.

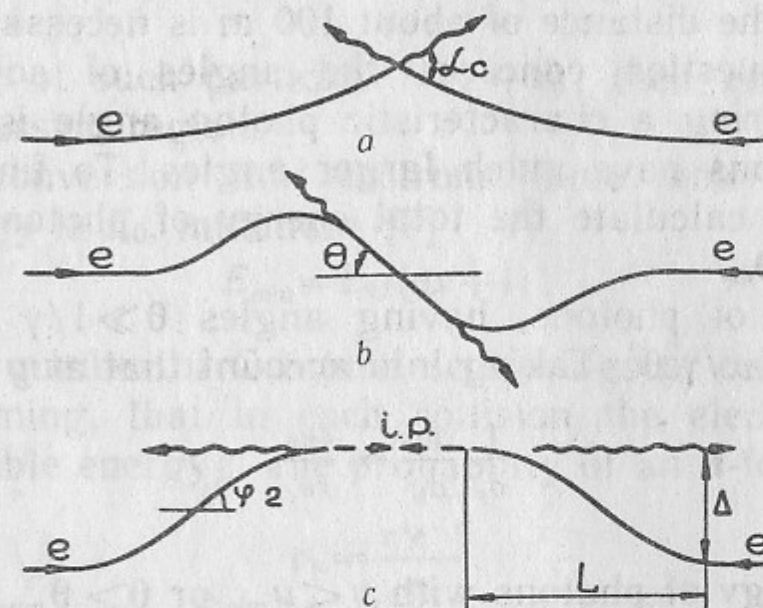


Fig. 10. Schemes of photon ejection.

At zero crossing angle  $\alpha_c$  one has to arrange a pass for photons between the i.p. and a beam absorber. This can be done in two ways.

1. The beam line is bent near the i.p., so that the collision axis has the angle  $\theta \neq 0$  relative to the collider axis (Fig. 10,b).

2. The interaction point is shifted some distance (of about 25 cm) relative to the collider axis, keeping  $\theta = 0$  (Fig. 10,c). In the first case there is again a problem with spin rotation. Let us consider the second scheme. The minimum distance  $L$  needed for misalignment of i.p. by  $\Delta \sim 25$  cm (for protection of the accelerator in the absorption region) is determined by the additional energy spread due to synchrotron radiation. This is important for the final focussing. Using the well known formulae for synchrotron radiation one can estimate the energy spread as follows:

$$\frac{\sigma_E}{E_0} \sim \frac{\sqrt{\Delta E \omega_c}}{E_0} \approx \frac{250 E_0^{5/2} (\text{TeV}) \varphi^{3/2}}{kL (\text{m})}, \quad (8.2)$$

where  $\omega_c$  is critical energy of synchrotron radiation,  $\varphi$  is the

bending angle,  $k$  is part of length with bending magnet. For VLEPP the energy spread of 0.3% is planned. Assuming an additional  $\sigma_E/E=0.2\%$ , and taking  $k=0.5$ ,  $\Delta=25$  cm and  $\varphi=4\Delta/L$ , we get  $L=125$  m and  $\varphi=0.008$ . The bending scheme must, of course, keep the emittance constant (as in SLC arcs).

This estimate can be used also for a nonzero crossing angle (basic scheme). It is seen, that to obtain the crossing angle  $\alpha_c/2=5$  mrad the distance of about 100 m is necessary.

The next question concerns the angles of soft photons. In Compton scattering a characteristic photon angle is  $\theta\sim 1/\gamma$ . However, soft photons have much larger angles. To find the required aperture let us calculate the total energy of photons travelling at the angles  $\theta>\theta_m$ .

The energy of photons, having angles  $\theta\gg 1/\gamma$  is found from eq. (5.1):  $\omega=E_0x/\gamma^2\theta^2$ . Taking into account that at  $y=\omega/E_0\ll 1$

$$\frac{1}{\sigma_c} \frac{d\sigma_c}{dy} = \frac{4\sigma_0}{x\sigma_c},$$

we get the energy of photons with  $y<y_{\min}$  or  $\theta>\theta_{\max}$ :

$$\frac{\Delta E}{E} = \int_0^{y_{\min}} \frac{y}{\sigma_c} \frac{d\sigma_c}{dy} dy \approx \frac{2\sigma_0 y_{\min}^2}{x\sigma_c} = \frac{2\sigma_0 x}{\sigma_c \gamma^4 \theta_{\max}^4}. \quad (8.3)$$

To provide  $\Delta E/E_0 < 10^{-8}$  at  $x\sim 5$  it is necessary to have  $\theta_{\max}\sim 200/\gamma$  i. e.  $\theta_{\max}\sim 10^{-4}$  at  $E_0=1$  TeV. This is the angular spread due to Compton effect only. The angular divergency of the electron beam should be added. In either case, the lense aperture will be larger, so that there are no serious problems with photon removal (especially for  $\alpha_c\neq 0$ , when photons travel outside the lenses). Note, that at  $\theta>700/\gamma\sim 3.5\cdot 10^{-4}$  the photons energies become less than 10 MeV, so that neutrons are not produced.

### 8.3. Removal of Electrons after Conversion

There are several sources of charged particles in  $\gamma\gamma$ -collisions:

- the initial electrons, which have not scattered in the conversion region;
- the electrons which have lost part of their energy at Compton scattering;
- electron-positron pairs, created under threshold [24, 25] (or

above that at  $x>4.8$ ) in the collision of the laser and high energy photons;

d) electron-positron pairs, created by photons at the i.p. in the field of the opposing deflected beam (and also in the field of separated  $e^+e^-$ -pairs).

There are also other sources, but they can be ignored in comparison with those enumerated. Let us consider the characteristics of these particles.

a). Number of such particles  $N(1-k)$ , their energy  $E_0$ , initial location—conversion region.

b). After conversion the electrons have wide spectrum. The maximum energy is  $E_0$ , minimum [7]

$$E_{\min}=E_0/(nx+1), \quad (8.4)$$

where  $n$  is the number of Compton scatterings of one and the same electron (assuming, that in each collision the electron losses the maximum possible energy). The probability of an  $n$ -fold collision

$$p_n = \frac{r^n e^{-r}}{n!}, \quad (8.5)$$

where  $n$ —probability of collision. Owing to the fact that after a few collisions the Compton cross section reaches the Thomson one  $\sigma_T=8\sigma_0/3$ , while in the beginning at  $x=5$   $\sigma_c=0.75\sigma_0$ , one can put  $r\approx 3.5r_0$  (a coef. of conversion  $k=1-\exp(-r_0)$ ,  $r_0=A/A_0$ ).

Let us estimate the minimum energy of particles to be considered, or such  $n$ , that  $E_{\min}p < 10^{-9}E_0$  (at lower level there are other backgrounds). Simple calculations give:  $n=13, 17, 24$  for  $r_0=0.5, 1, 2$  ( $k=0.4, 0.63, 0.86$ ) and, correspondingly,  $E_{\min}=1.5\%, 1.2\%, 0.8\%$  of  $E_0$ . In fact, soft electrons lose in average two times less energy than at maximum transfer, therefore the result must be increased by a factor 2. For further calculation we assume  $E_{\min}/E_0=2\%$ .

c). The number of  $e^+e^-$ -pairs created in the conversion region can account for a notable amount even below threshold  $x=4.8$  [24, 25]. At the beginning these particles have the energies of  $E_0/2$ . However, as a result of multiple collisions, their energy will drop, as in the preceding case, down to  $2\% E_0$ . The initial position of these particles is the conversion region.

d). These pairs are created at the i.p. Their amount is little at  $\gamma_1 < 1$  and can be compared with the number of photons at large  $\gamma_1$ . Minimum energy of these particles is  $\sim 0.2E_0/\gamma_1$ .

All these particles are deflected in the fields of the bending magnets and opposing beam. As a result, particles have some energy spread mostly in the horizontal plane.

Let us calculate the angles of particles going out from the conversion region, Fig. 7. At first a particle with the energy  $E$  passes the bending magnet, where it acquires the angle

$$\alpha_m = eB_e b / E. \quad (8.6)$$

At the i.p. it has the displacement

$$x = eB_e b^2 / 2E. \quad (8.7)$$

Let us find now the deflection angle in a collision with opposing beam. The main influence comes from the particles with energy  $E_0$ , since they are closer to the axis. If the impact parameter changes not too much during the collision (upper limit), deflection angles are

$$\alpha_b = \frac{2e^2 N(1-k)}{E(x_0+x)}, \quad (8.8)$$

where  $x_0$  is the displacement of particles with the energy  $E_0$  (eq. (8.7)).

It is of interest, that angles  $\alpha_b$  for various energies differ less, than by a factor 2. It is because the particles with smaller energy come to the i.p. with larger displacement. The resulting deflection angle in the field of the two magnets with the same direction and the field of the opposing beam is

$$\begin{aligned} \alpha_{tot} &= \alpha_b + 2\alpha_m \quad \text{for } e^-, \\ \alpha_{tot} &= \alpha_b - 2\alpha_m \quad \text{for } e^+ \end{aligned}$$

(at  $x < 4.8$  some amount of  $e^+$  is produced due to nonlinear effects in conversion region).

Substituting to  $\alpha_m$  and  $\alpha_b$  values of  $x$  and  $b$  from the formulae (7.10) — (7.13) at  $p_1 < 0.1$ , i. e.  $\Upsilon_1 \sim 1$ , we get

$$\alpha_m = \frac{E_0}{E} \sqrt{\frac{4N(1-k) B_e r_e}{\sigma_z B_0}}, \quad (8.9)$$

$$\alpha_b = \frac{\alpha \sigma_z}{\gamma^2 r_e} \frac{1}{1+E/E_0}. \quad (8.10)$$

So, at  $k=0.5$ ,  $B_e=30$  kGs, the deflection angles for particles with energies  $E=(E_0 \div 0.02E_0)$  account for:

$$\begin{aligned} \text{VLEPP: } \alpha_m &= (0.03 \div 1.5) \cdot 10^{-3}, & \alpha_b &= (2.5 \div 5) \cdot 10^{-4}, \\ \text{TLC: } \alpha_m &= (0.025 \div 1.4) \cdot 10^{-3}, & \alpha_b &= (1 \div 2) \cdot 10^{-4}. \end{aligned} \quad (8.11)$$

We see that these deflection angles are not large enough to enable particles to travel out of the lense aperture in the case of head-on collision (see Sect. 9). But, if beams collide at crossing angle  $\alpha_c \sim (5-10) \cdot 10^{-3} > 2\alpha_m + \alpha_b$  then all the particles will pass out of the lenses.

As was already discussed before, we will not consider here in detail the case of intensive pair production. Note only that at  $\Upsilon_1 \gg 1$  many soft particles are created in the field of the opposing beam and they follow a way in the same strong field (unlike particles going from the conversion region). Therefore, they have large deflection angles, that make the removal problem more difficult.

Formulae (8.9) — (8.11) were obtained for  $\Upsilon_1=1$ , when is noticeable pair creation probability. However, in this case the produced particles are hard enough ( $E > 0.25E_0$ ) and their deflection angles do not come out of the range (8.11).

Bending magnets must also be considered. The distance between conversion region and i.p. at  $\Upsilon_1=1$  (7.13) for TLC and VLEPP are 1.5 and 3.5 cm respectively (at  $B_e=30$  kGs). The gap of the magnet has to be large enough to let pass the laser beam. We assume also, that laser shines at  $\alpha_0=0$ . If we take angular aperture  $\Delta\alpha = \pm 2.5\alpha_\gamma$ , then  $d > 10b\alpha_\gamma$  (it is accounted, that light pass by both magnets). Substituting from (5.9)  $\alpha_\gamma = 3 \cdot 10^{-2}$  (for  $x=4.8$ ) and at  $b=3.5$  cm, we find  $d \sim 1$  cm. It was supposed everywhere above, that bending field begins just from the i.p, so that no free space was reserved for outgoing products of reactions (which we are going to explore). This can be easily taken in to account. However, in principle, one can build a superconducting magnet with a thickness of walls less than 0.1 radiation length and with  $B_e \geq 30$  kGs. Such the magnets can be allowed to surround i.p. from all sides.

Resume. For colliders of TeV energy removal of particles from conversion and interaction regions can be done in simplest way if to collide beams at crossing angle  $\alpha_c \sim 10$  mrad. The «crab crossing» scheme makes it possible.

## 9. FINAL FOCUSING

### 9.1. Emittance and Beam Sizes

The transverse size of photon beam is determined by Compton scattering ( $\sim b/\gamma$ ), and the size of the electron bunch  $a$ . A natural requirement in the size of the electron bunch is  $a \sim b/\gamma$ . Let us consider real possibilities.

In space between lenses the beam size in the  $i$  ( $i=x, y$ )-direction varies in the following way (see Sect. 2.3)

$$\sigma_i = a_i \sqrt{1 + \frac{z^2}{\beta_i^2}}. \quad (9.1)$$

The r.m.s beam size at interaction point

$$a_i = \sqrt{\varepsilon_{ni} \beta_i / \gamma}, \quad (9.2)$$

where  $\varepsilon_{ni}$  is the normalized emittance,  $\beta_i$ —beta-function (min ( $\beta_i$ )  $\sim \sigma_z$ ).

From here follows the requirements on the beam emittance

$$\varepsilon_{ni} \sim b^2 / \gamma \beta_i. \quad (9.3)$$

As was already discussed, for TeV colliders one can put  $\Upsilon_1 \sim 1$ . Then according to (7.13),

$$\frac{b^2}{\gamma^2} = \frac{4N(1-k)r_e^3 B_0}{\alpha^2 \sigma_z B_e}. \quad (9.4)$$

Substituting (9.4) into (9.3), we get

$$\varepsilon_{ni} = \frac{4N(1-k)r_e^3 \gamma B_0}{\alpha^2 \sigma_z \beta_i B_e}. \quad (9.5)$$

At  $k=0.5$ ,  $B_e=30$  kGs and  $\beta_i=\sigma_z$ , we get

$$\begin{array}{ll} \text{VLEPP:} & \varepsilon_{ni} \approx 9 \cdot 10^{-5} \text{ cm} \cdot \text{rad}, \\ \text{TLC:} & \varepsilon_{ni} \approx 3.5 \cdot 10^{-4} \text{ cm} \cdot \text{rad}. \end{array} \quad (9.6)$$

In these estimations an essential effect was not taken in to account: chromatic aberration of lenses (that is, the focal distance of a lens depends on the particle energy). There are two sorts of chromaticity. The first one is connected with the energy spread of

the beam at the entrance of the focussing system. This can be corrected (in a certain limit). In the second case an additional energy spread arises at the final stage of focussing in the field of the lens itself (effect K. Oide). Here nothing can be done. Let us consider the requirements on emittance due to the latter effect.

$$a_i^2 \approx \frac{\varepsilon_{ni} \beta_i}{\gamma} \left( 1 + \frac{F^2}{\beta_i^2} \frac{\sigma_E^2}{E_0^2} \right), \quad (9.7)$$

where  $F$  is the focal distance. The energy spread arising in lenses, (see eq. (8.2))

$$\frac{\sigma_E}{E_0} \approx \frac{2.5 \cdot 10^4 E_0^{5/2} (\text{TeV}) \alpha^{3/2}}{l (\text{cm})}, \quad (9.8)$$

where  $l$ —length of lens. The bending angle in the lens

$$\alpha_i \sim \sqrt{\frac{\varepsilon_{ni}}{\beta_i \gamma}}. \quad (9.9)$$

Assuming  $F \sim 2l$  from (9.7) — (9.9), we get

$$a_i^2 \approx \frac{\varepsilon_{ni} \beta_i}{\gamma} + \varepsilon_{ni}^{5/2} \beta_i^{-5/2} \gamma^{5/2} \cdot 10^{-22}. \quad (9.10)$$

The maximum is reached at

$$\beta_i = \gamma \varepsilon_{ni}^{3/7} \cdot 6.7 \cdot 10^{-7}, \text{ cm}. \quad (9.11)$$

Then

$$a_i \approx 1.2 \sqrt{\frac{\varepsilon_{ni} \beta_i}{\gamma}} \approx 10^{-3} \varepsilon_{ni}^{5/7}, \text{ cm}. \quad (9.12)$$

Assuming  $a_i = b/\gamma$ , we get

$$\varepsilon_{ni} = 1.5 \cdot 10^4 \left( \frac{b}{\gamma} \right)^{7/5}, \text{ cm} \cdot \text{rad}, \quad (9.13)$$

$$\beta_i = 85 \left( \frac{b}{\gamma} \right)^{3/5} \cdot E_0 (\text{TeV}), \text{ cm}. \quad (9.14)$$

These formulae are valid, when  $\beta_i > \sigma_z$ . Otherwise one has to take  $\beta_i \approx \sigma_z$  and use the eq. (9.5). From here, taking into account (9.4), we get for TLC at  $k=0.5$

$$\beta_i \approx 0.025 E_0 \text{ (TeV), cm} \quad \text{and} \quad \varepsilon_{ni} \approx 10^{-4} \text{ cm} \cdot \text{rad.} \quad (9.15)$$

For VLEPP at  $E_0=1$  TeV the estimates (9.6) are valid, i. e.  $\beta_i \sim 0.075$  cm and  $\varepsilon_{ni} \sim 10^{-4}$  cm·rad. We see, that the requirements are close enough.

In the damping ring is naturally obtained  $\varepsilon_{ny} \ll \varepsilon_{nx}$ . Preliminary analysis shows [27], that it is rather real to obtain the emittance of  $\varepsilon_{nx} \sim 10^{-4}$  cm·rad. To what extent this normalized emittance will be saved during acceleration in collider—it is difficult question and there is no clear answer yet.

Let us consider now chromatic errors, due to beam energy spread before lenses. We are going to correct it, but not completely. The ratio of beam size due to chromaticity to that without energy spread is (comp. (9.7))

$$\frac{(a_i)_{ch}}{a_i} \sim \frac{F}{\beta_i} \frac{\sigma_E}{E} \quad (9.16)$$

For  $F=200$  cm,  $\beta_i = \sigma_z = 0.075$  cm,  $\sigma_E/E = 0.3\%$  we get  $(a_i)_{ch}/a_i = 8$ . A chromaticity of lenses can be corrected by dispersion of the beam and use of sextupole lenses. The most simple way is to make a correction only in the  $x$  direction and do nothing in  $y$ , because of  $\varepsilon_{ny} \ll \varepsilon_{nx}$ . The minimum beam size on  $y$  in this case takes place at

$$\beta_y \sim F \frac{\sigma_E}{E} \quad (9.17)$$

and equals

$$a_y = \sqrt{2\varepsilon_{ny}\beta_y/\gamma} \quad (9.18)$$

Ratio of beam sizes

$$1/R = a_y/a_x = \sqrt{\frac{2F}{\beta_x} \frac{\sigma_E}{E_0}} \sqrt{\frac{\varepsilon_{ny}}{\varepsilon_{nx}}} \quad (9.19)$$

For example given above we have  $R=1$  at  $\varepsilon_{ny} \sim 0.06\varepsilon_{nx}$ . For further estimation we adopt for

$$a \equiv \sqrt{2} \quad a_x = \sqrt{2} \quad a_y = b/\gamma \quad (9.20)$$

The characteristic values:

Table 2

	$a$ , cm	$x_0$ , cm	$b$ , cm
VLEPP	$1.8 \cdot 10^{-6}$	$6 \cdot 10^{-5}$	3.5
TLC	$1.5 \cdot 10^{-6}$	$2.2 \cdot 10^{-5}$	1.5

It is easy to make sure, that in the conversion region the electron beam size is much smaller than that of the laser, as was assumed in Sect. 5.2 at the calculation of the laser flash energy.

## 9.2. The Requirements on Focussing Lenses

In distinction from  $e^+e^-$ -collisions, where flat beams are used, in  $\gamma\gamma$ -collisions the ultimate focussing on the horizontal direction is necessary also. Let us estimate the required parameters of lenses: gradient  $G$ , length  $l$ , field on poles  $B_{\max}$ , aperture  $R_l$ . Numerical examples are given for VLEPP.

### Gradient

The bending angle in a lens

$$\alpha \sim l/R, \quad (9.21)$$

where  $R$  is a radius of curvature

$$R = E_0/eGF\alpha. \quad (9.22)$$

Hence

$$G \sim \frac{E_0}{elF} = \frac{3.3 \cdot 10^{16} E_0 \text{ (TeV)}}{l \text{ (cm)} F \text{ (cm)}} \frac{\text{kGs}}{\text{cm}} \quad (9.23)$$

Focal length can not be done too large, for it will be difficult to correct the chromatic aberration (9.16). At  $\sigma_E/E_0 = 0.3\%$  a reasonable limit is  $F \sim 200$  cm. Assuming  $l = 0.5 \cdot F = 100$  cm for  $E_0 = 1$  TeV we get  $G = 160$  kGs/cm.

### Aperture

R.m.s. beam size in lens

$$\sigma_x \sim F \sqrt{\varepsilon_{nx}/\gamma\beta_x}, \quad \beta_x \sim \sigma_z \quad \text{or} \quad (9.14); \quad (9.24)$$

$$\sigma_y \sim F \sqrt{\varepsilon_{ny}/\gamma\beta_y}, \quad \beta_y \sim F \frac{\sigma_E}{E}. \quad (9.25)$$



At  $F=200$  cm,  $\varepsilon_{nx}=10^{-4}$  cm·rad,  $\varepsilon_{ny}=0.06\varepsilon_{nx}$  (see (9.19)),  $\sigma_E/E_0=0.3\%$ ,  $E_0=1$  TeV one gets

$$\sigma_x \sim 5 \cdot 10^{-3} \text{ cm},$$

$$\sigma_y \sim 5 \cdot 10^{-4} \text{ cm},$$

i. e. the electron beam is flat in lenses.

**The required aperture**

$$R_l \sim 10 \sigma_x \approx 10 \sqrt{\frac{\varepsilon_{nx}}{\gamma\beta_x}} F \sim 5 \cdot 10^{-2}, \text{ cm (for VLEPP)}. \quad (9.26)$$

**Field on poles**

The maximum field in lenses

$$B_{\max} \sim GR_l = \frac{10}{el} \sqrt{\frac{\varepsilon_{nx} E_0 m c^2}{\beta_x}}. \quad (9.27)$$

For VLEPP (see parameters above)  $B_{\max} \sim 10$  kGs, i. e. iron lenses can be used.

All these estimates are, of course, very approximate.

## 10. LUMINOSITY, MONOCHROMATICITY

For round beams formulae for spectral luminosities of  $\gamma\gamma$ - and  $\gamma e$ -collisions were derived in Ref. [7, 10]. Here we will analyze once again a dependance of a total luminosity and monochromaticity on various parameters, and find out their values for the considered schemes. The monochromaticity  $n_{\gamma\gamma}$  we define as a ratio of the range of invariant mass  $\Delta W_{\gamma\gamma}$ , that contains half of the luminosity to  $W_{\gamma\gamma, \max}$ . The monochromaticity depends on the parameter

$$\rho^2 = \left(\frac{b}{\gamma a}\right)^2, \quad (10.1)$$

where, as before,  $b$  is the distance between conversion region and i.p.,  $a$  is the r.m.s. radius of electron beam at i.p. Note, that in Ref. [7, 10] was used  $\rho^2$  larger by a factor  $x+1$ . In the new definition  $\rho^2$  does not depend on  $x$ , that is more convenient for clarifying the dependence of the luminosity and monochromaticity on laser wave length.

The luminosity is presented in a ratio to

$$L_{ee} = \frac{N^2 f}{2\pi a^2}. \quad (10.2)$$

For round beams the distribution of luminosity on invariant mass of  $\gamma\gamma$ -system  $W_{\gamma\gamma}$  has a form [7, 10]

$$\frac{dL_{\gamma\gamma}}{dz} = 2zk^2 L_{ee} \int_{z^2/y_m}^{y_m} f(x, y) f\left(x, \frac{z^2}{y}\right) I_0(\rho^2(x+1)) \sqrt{\left(\frac{y_m}{y}-1\right)\left(\frac{y_m y}{z^2}-1\right)} \times \\ \times \exp\left[-\left(\frac{y_m}{y} + \frac{y_m y}{z^2} - 2\right) \frac{(x+1)\rho^2}{2}\right] \frac{dy}{y}, \quad (10.3)$$

where  $z = W_{\gamma\gamma}/2E_0$ ,  $\rho = b/\gamma a$ ,  $f(x, y)$  is defined in (5.2),  $I_0(x)$  is the Bessel function for an imaginary argument. The total luminosity

$$L_{\gamma\gamma} = \int_0^{z_{\max}} \frac{dL_{\gamma\gamma}}{dz} dz, \quad \text{where } z_{\max} = \frac{x}{x+1}.$$

In Fig. 11 the plots of spectral luminosities are shown for unpolarized and polarized beams ( $2P_e \lambda = -1$  both beams). Polarization

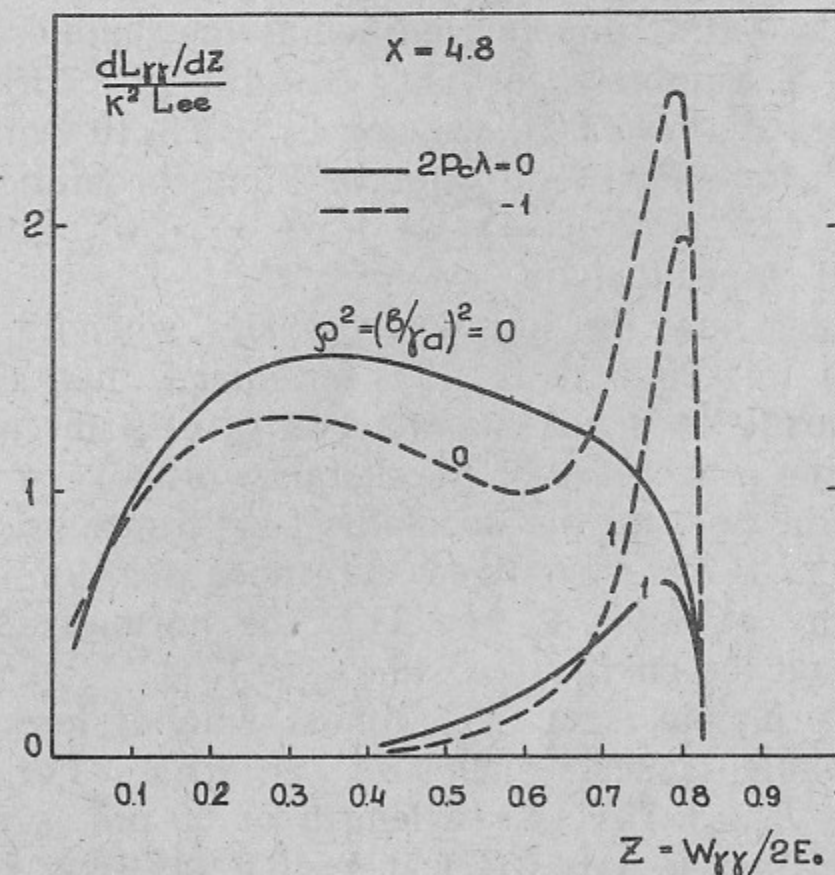


Fig. 11. Spectral luminosity of  $\gamma\gamma$ -collision.

improves monochromaticity. With growth of  $\rho^2$  collisions become more and more monochromatic, since photons with higher energies collide on smaller spot size and, therefore, contribute more to the luminosity (at  $\rho^2=0$  all the energies are mixed). The dependence of monochromaticity on  $\rho^2$  is shown in Fig. 12,b. Polarization improves monochromaticity approximately twice as much, while increasing  $x$  from 4.8 to 20—by a factor 2.5. The dependence of the total luminosity on  $\rho^2$  is depicted in Fig. 12,a. At  $2P_c\lambda=-1$  the luminosity is higher than for unpolarized beams by a factor  $1.5 \div 2$  at  $\rho^2 > 1$ , and as soon as monochromaticity is also better, then  $dL/dz$  is higher in 3-4 times. Increasing of  $x$  from 4.8 to 20 leads to some drop of the luminosity, but due to monochromaticity  $dL/dz$  is still higher at  $x=20$  twice as much. However, recalling, that at  $x > 4.8$  the maximum conversion coefficient is 0.25, and  $L_{\gamma\gamma} \propto k^2/(1-k)$  (7.16), then by this item it is also profitable to work at  $x < 4.8$ .

Let us find out the  $\gamma\gamma$ -luminosity at VLEPP for the scheme considered in the previous section, namely:  $E_0=1$  TeV,  $k=0.5$ ,  $b \sim 4$  cm,  $a=2 \cdot 10^{-6}$  cm, (i. e.  $\rho^2=1$ ),  $N=2 \cdot 10^{11}$ ,  $f=10^2$ . For  $x=4.8$  and  $2P_c\lambda=-1$  we find out from Fig. 12,a, that  $L_{\gamma\gamma}=0.22 \cdot k^2 L_{ee}$ , where  $L_{ee}$  is defined by (10.2). From here  $L_{\gamma\gamma}=9 \cdot 10^{33} \text{ cm}^{-2} \text{ s}^{-1}$ . For unpolarized beams the luminosity is smaller by a factor 1.5. Similarly, for TLC ( $a=1.5 \cdot 10^{-6}$  cm,  $b=1.5$  cm ( $\rho^2=1$ ),  $N=1.4 \cdot 10^{10}$ ,  $f=3.600$ , we get  $L_{\gamma\gamma}=2.8 \cdot 10^{33} \text{ cm}^{-2} \text{ s}^{-1}$  and  $1.9 \cdot 10^{33} \text{ cm}^{-2} \text{ s}^{-1}$  for  $2P_c\lambda=-1$  and 0. Monochromaticity can be found from Fig. 12,b. For  $\rho^2=1$  we have  $\eta_{\gamma\gamma} \sim 8\%$  and  $15\%$  for  $2P_c\lambda=-1$  and 0 respectively.

Let us consider how the luminosity varies when the energy is decreased from 1 to 0.25 TeV. If all is optimized, then according to (7.16) the luminosity does not change. For VLEPP the optimization at 0.25 GeV means a decrease of the distance  $b$  between the conversion region and the i.p. and the normalized emittance both by a factor 4 (eq. (9.5)). With unchanged emittance the luminosity will drop less than by a factor 4. For TLC the normalized emittance does not depend on the energy (eq. (9.4), (9.13)).

One can, in principle, scan  $W_{\gamma\gamma}$  almost without loss of luminosity using tunable laser, such as a FEL. For obtaining  $W_{\gamma\gamma}=0.5$  TeV at  $E_0=1$  TeV, wave length of  $60 \mu\text{m}$  is needed and the energy of the flash is only 0.3 J at  $k=0.5$  (as soon as  $\sigma_c \approx \sigma_T$ ).

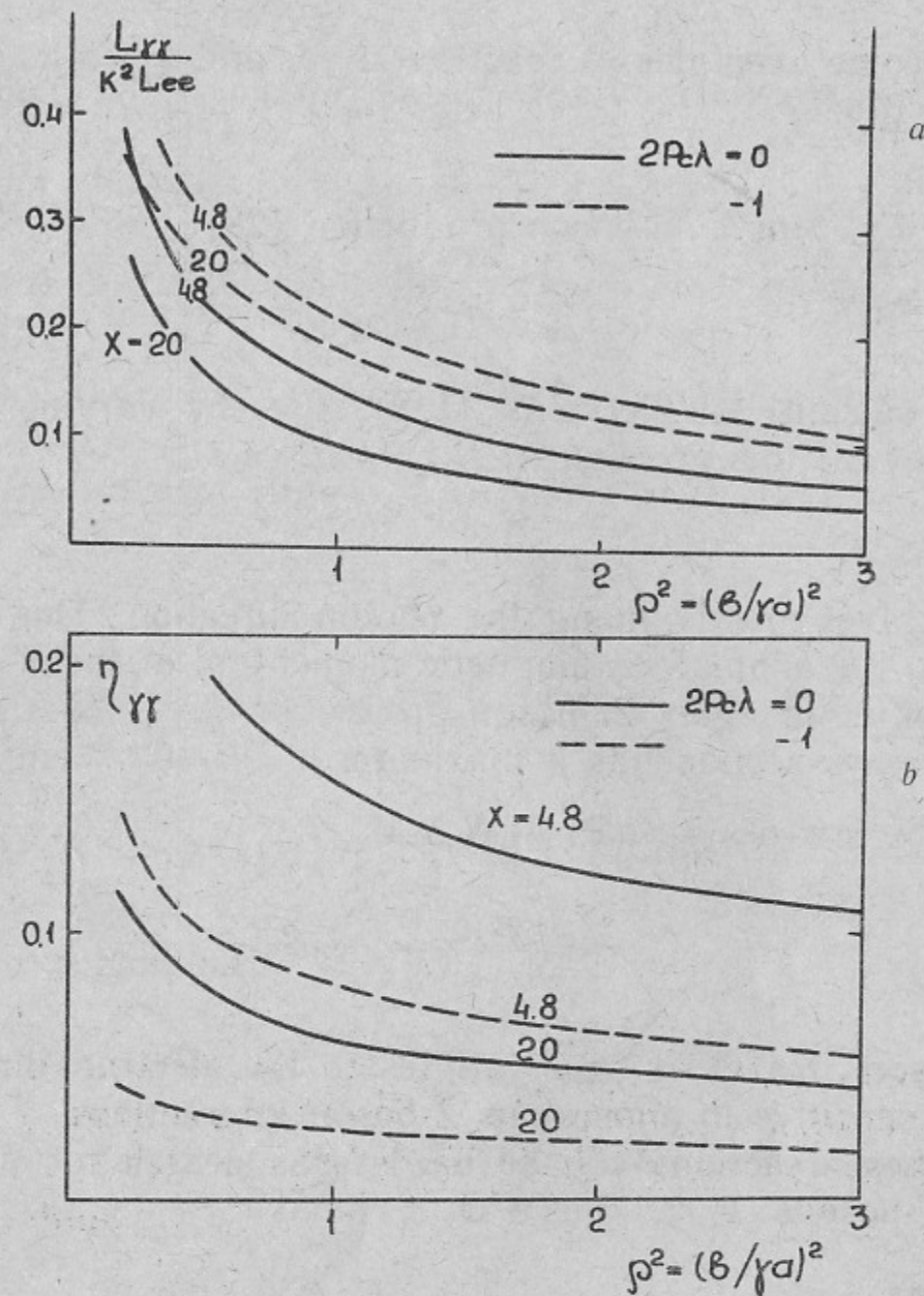


Fig. 12. a— dependence of the total  $\gamma\gamma$ -luminosity on  $\rho^2$ , b—dependence of monochromaticity on  $\rho^2$ .

## 11. CHARACTERISTIC CROSS SECTIONS OF PROCESSES

Below some examples of reaction in  $\gamma e$ - and  $\gamma\gamma$ -collisions at high energy are given.

### $\gamma e$ -collisions

1.  $\gamma e \rightarrow W\nu$ . Single  $W$ -boson production [28]. Cross section of the reaction

$$\sigma_{\gamma e \rightarrow W\nu} = (1 - 2\lambda) \sigma^{np}, \quad (11.1)$$

where  $\lambda$ —spirality of electrons (1/2). I. e. by varying  $\lambda$  one can switch on or off this process. At  $S_{\gamma e} = 4\omega E_0 \gg M_W^2$

$$\sigma^{np} = 47 \cdot 10^{-36} \text{ cm}^2. \quad (11.2)$$

$W$ -boson travel mostly along the photon direction. This reaction is sensitive to the anomalous magnetic momentum of the  $W$ -boson.

2.  $\gamma e \rightarrow Z_0 e$ . «Single»  $Z_0$ -boson production [28]. Just above threshold the cross section has a maximum of  $90 \cdot 10^{-36} \text{ cm}^2$ , then falls down by the low  $\sigma \propto \frac{1}{S} \ln S$ . At  $S \gg M_{Z_0}^2$

$$\sigma \sim \frac{1.2 \cdot 10^{-36}}{S_{\gamma e} (\text{TeV}^2)}, \text{ cm}^2 \quad (11.3)$$

and  $Z_0$ -bosons travel at small angles to the electron direction. The process is sensitive to anomalous  $Z$ -boson interactions.

Both these reactions can be used for a search for nonstandard  $W$ - and  $Z_0$ -bosons.

### $\gamma\gamma$ -collisions

1. The total cross section  $\gamma\gamma \rightarrow \text{hadrons}$  does not fall with energy and is approximately  $\sim 3 \cdot 10^{-31} \text{ cm}^2$ . Reaction products travel predominantly forward, as in hadron-hadron collisions. Many such events per collision will take place.

2.  $\gamma\gamma \rightarrow W^+ W^-$  [28]. At  $S > M_W^2$  the cross section tends to  $\sigma = \text{const} = 86 \cdot 10^{-36} \text{ cm}^2$ . The reaction allows one to investigate vertices  $\gamma WW$ ,  $\gamma\gamma WW$ . The cross section is sensitive to the anomalous magnetic moment of the  $W$ -boson.

3.  $\gamma\gamma \rightarrow H^+ H^-$  (pair of scalars, charged Higgs, for example). At  $S \gg M_H^2$

$$\sigma_{\gamma\gamma \rightarrow H^+ H^-} \sim \frac{2\pi\alpha^2}{S} = 1.5 \sigma_{e^+ e^- \rightarrow \mu^+ \mu^-} = \frac{1.2 \cdot 10^{-37}}{S (\text{TeV}^2)}, \text{ cm}^2. \quad (11.4)$$

Note, that  $\sigma_{\gamma\gamma \rightarrow H^+ H^-} = 6\sigma_{e^+ e^- \rightarrow \mu^+ \mu^-}$  (only electromagnetic production)

4.  $\gamma\gamma \rightarrow L^+ L^-$  (pair of leptons). At  $S \gg M_L^2$

$$\sigma_{\gamma\gamma \rightarrow L^+ L^-} \approx \frac{4\pi\alpha^2}{S} \ln \frac{S}{4M_L^2} \approx 3 \ln \frac{S}{4M_L^2} \sigma_{e^+ e^- \rightarrow L^+ L^-} \sim \frac{5 \cdot 10^{-37}}{S (\text{TeV}^2)}, \text{ cm}^2. \quad (11.5)$$

We see, that for standard electrodynamic processes 3, 4  $\sigma_{\gamma\gamma} / \sigma_{e^+ e^-} \sim 3 \div 6$ .

5.  $\gamma\gamma \rightarrow H_0$  (neutral Higgs). Full width of  $H_0$  [29] at  $M_{H_0} \gg M_W$

$$\Gamma_{\text{tot}} = \frac{3GM_H^3}{16\pi\sqrt{2}} = 0.5 M_H^3 (\text{TeV}), \text{ TeV} \quad (11.6)$$

and account for  $\sim 0.1 M_H$  at  $M_H = 0.5 \text{ TeV}$ . Two photon width is equal [30]

$$\Gamma_{H_0 \rightarrow \gamma\gamma} = \left(\frac{\alpha}{2\pi}\right)^2 \frac{GM_H^2}{8\pi\sqrt{2}} = 0.45 M_H^3 (\text{TeV}), \text{ MeV}. \quad (11.7)$$

At resonance maximum

$$\sigma_{\gamma\gamma \rightarrow H_0} = \frac{8\pi\Gamma_{\gamma\gamma}}{M_H^2\Gamma} = \frac{0.75 \cdot 10^{-38}}{M_H^2 (\text{TeV})}, \text{ cm}^2, \quad (11.8)$$

that is  $3 \cdot 10^{-38} \text{ cm}^2$  at  $M_H = 0.5 \text{ TeV}$ . This formula works, when  $\eta_{\gamma\gamma} < \Gamma/M$ , i. e. at  $M_H > 0.5 \text{ TeV}$ . For smaller  $M_H$  the effective cross section will be

$$\sigma_{\gamma\gamma \rightarrow H_0}^{ef} \approx \frac{dL_{\gamma\gamma}}{dzL_{\gamma\gamma}} \frac{2\pi^2\Gamma_{\gamma\gamma}}{M_H^3} \approx \frac{3 \cdot 10^{-39}}{\eta_{\gamma\gamma}} \approx 3 \cdot 10^{-38} \text{ cm}^2. \quad (11.9)$$

In thirty percent of the cases,  $H_0$  decays into  $Z_0 Z_0$ . This mode has the best condition for a search of  $H_0$ , as it dominates in  $\gamma\gamma \rightarrow Z_0 Z_0$ .

The number of events per  $10^7 \text{ s}$  (1/3 of a year) at  $L_{\gamma\gamma} = 5 \cdot 10^{33}$  and  $L_{\gamma e} = 5 \cdot 10^{32} \text{ cm}^{-2} \text{ s}^{-1}$  at  $E_0 = 1 \text{ TeV}$  is given in Table 3. For a reaction  $\gamma\gamma \rightarrow H_0$  ( $M = 0.5 \text{ TeV}/c^2$ )  $L_{\gamma\gamma} = 2 \cdot 10^{33}$  is taken, due to lower energy (see remarks at the end of Sect. 10).

It can be added, that Higgs production occurs via a loop with a  $W$ -boson. If it is a composite particle, then  $\Gamma_{\gamma\gamma}$  may be larger by many orders [31, 13]

Table 3

Process	Number of events
$\gamma e \rightarrow W \nu$	$2.5 \cdot 10^5$
$\gamma e \rightarrow Z_0 e$	$1.5 \cdot 10^3$
$\gamma \gamma \rightarrow W^+ W^-$	$2 \cdot 10^6$
$\gamma \gamma \rightarrow H^+ H^-$	$1.5 \cdot 10^3$
$\gamma \gamma \rightarrow L^+ L^-$	$5 \cdot 10^3$
$\gamma \gamma \rightarrow H_0$	500

## CONCLUSION

Principal problems of  $\gamma\gamma$  and  $\gamma e$  colliding beams at linear colliders have been considered.

Special attention was devoted to beam collision effects, restricting luminosity. For  $\gamma\gamma$ -collisions there is only one principle collision effect—coherent pair creation by photons in the field of an opposing bunch, deflected after passage of the conversion region. For planned one TeV colliders the restriction arises only at  $L_{\gamma\gamma} > 10^{34} \text{ cm}^{-2} \text{ s}^{-1}$ , which exceeds the attainable  $L_{e^+e^-}$ .

In  $\gamma e$ -collisions, the decisive effects are coherent pair creation by the photons in the field of main electron beam and beamstrahlung losses of electrons in the field of opposing beam deflected after conversion. At the same colliders  $L_{\gamma e}$  is restricted by these effects to the level  $< 5 \cdot 10^{32} \text{ cm}^{-2} \text{ s}^{-1}$ . For detailed exploration of  $\gamma e$ -physics in the TeV region such a value of luminosity is not enough, but for  $E_0$  of a few hundreds GeV it is good enough, since with a decrease of energy the cross sections and limit on luminosity grow (7.35), (7.36).

Removal of particles from conversion and interaction regions can be done in the simplest way using the «crab» scheme with the crossing angle of 10 mrad.

The normalized emittance of the electron beam has to be  $\varepsilon_{nx} \sim 10^{-4} \text{ cm} \cdot \text{rad}$  and  $\varepsilon_{ny} < 0.1 \varepsilon_{nx}$ .

For obtaining conversion coefficient  $k=0.5$  the laser with flash energy of about 2 J and time duration of 10 ps is required. Optimum wave length  $\lambda = 4.5 \cdot E_0$  (TeV),  $\mu\text{m}$ . It is desirable to have a tunable laser, FEL for example, in the range  $1 \div 50 \mu\text{m}$ .

Taking into account all limitations of principal and technical character, the  $L_{\gamma\gamma}$  possible at designed colliders is of the order of  $(0.5 \div 1) \cdot 10^{34} \text{ cm}^{-2} \text{ s}^{-1}$ . The processes which can be studied here are not less interesting, than those proposed in  $e^+e^-$ -collisions.

This opportunity undoubtedly has to be taken into account in the design of future linear colliders.

I am very grateful to I.F. Ginzburg, G.L. Kotkin, V.G. Serbo for joint work on principles of the method, to P. Chen for cooperation on coherent pair production and also to V.E. Balakin, P.M. Ivanov, I.A. Koop, A.A. Mikhailichenko, V.V. Parkhomchuk, A.N. Skrinsky, N.A. Solyak, A.A. Zholents for helpful discussions.

## REFERENCES

1. V. Balakin, G. Budker, A. Skrinsky. Problems of High Energy Physics and Therm. Nucl. Synthesis.—Novosibirsk: Nauka, 1978; Preprint INF 78-101, Novosibirsk, 1978.  
V. Balakin and A. Skrinsky. Proc. Second ICFA Workshop on Possibilities and Limitations of Accelerators and Detectors, Les Diablerets, 1979, p.31.  
N. Solyak. Preprint INF 88-44. Novosibirsk, 1988.
2. W. Schnell. (CLIC) ICFA-3 Proceedings, Brookhaven, 1987, p.200.
3. R. Ruth. ICFA-3 SLAC-PUB-4848, 1989.
4. M. Yoshioka. Report at Inter. Work. on Next Generation of Linear Colliders, December 1988, SLAC. (The flat beams are discussed for JLC as well.)
5. I. Ginzburg, G. Kotkin, V. Serbo, V. Telnov. Pis'ma v ZhETF, 34 (1981) 514 (Preprint INF 81-50, Novosibirsk, 1981).
6. C. Akerlof. Preprint UMHE 81-59, Univ. of Michigan, 1981.
7. I. Ginzburg, G. Kotkin, V. Serbo, V. Telnov. Nucl. Instr. Meth., 205 (1983) 47.
8. V. Balakin, A. Skrinsky. Preprint INF 81-129, Novosibirsk, 1981.  
A. Skrinsky. Uspekhi Fiz. Nauk, 138 (1982) 3.
9. A. Kondratenko, E. Pakhtusova, E. Saldin. Dokl. Akad. Nauk, 264 (1982) 849 (Russian).
10. I. Ginzburg, G. Kotkin, S.L. Panfil, V. Serbo, V. Telnov. Nucl. Instr. and Meth., 219 (1984) 5.  
I. Ginzburg, G. Kotkin, V. Serbo, V. Telnov. Yadernay Fizika, v.38, 2 (8) (1983) 372.
11. J.E. Spencer. SLAC-PUB-3645 (1985).
12. F. Renard. Proc. of the VII Int. Workshop on Photon-Photon Collisions, Paris, 1986.
13. I. Ginzburg, V. Serbo. Materialy XXIII Zimney Shkoly LIYF, 1988, p.137 (Russian).
14. V. Balakin, N. Solyak. Preprint INF 82-123. Novosibirsk, 1982; Proc. of VIII All Union Work on Char. Part. Accel., Dubna, 1983, v.2, p.263 (Russian); Proc. of VIII Intern Conf. on High Ener. Accel., Novosibirsk, 1987, p.151.  
N. Solyak. Preprint INF 88-44. Novosibirsk, 1988.

15. *R. Noble*. Nucl. Instr. and Meth., A256 (1987) 427 and ref. there.
16. *U. Amaldi*. CERN-EP/87-169, Lecture at US-CERN School on Part. Accel., South Padre, Texas, 1986 and ref. there.
17. *F.R. Arutyunian and V.A. Tumanian*. Phys. Lett., 4 (1963) 176;  
*R.H. Milburn*. Phys. Rev. Lett., 10 (1963) 75.
18. *T. Vsevolozhskaya et al.* Proc. of the XIII Inter. Conf. on High Energy Accel., Novosibirsk, 1987, p.164.
19. *V. Balakin et al.* ICFA-3 Proceedings, p.244, Brookhaven, 1987.
20. *J. Fraser et al.* Proc. of 1987 Part. Accelerator Conf., Washington, 1987 and ref. therein.
21. *A. Fasso et al.* CERN 84-02, 1984.
22. *V. Budnev, I. Ginzburg, G. Meledin, V. Serbo*. Phys. Rep. 15C (1975) 181.
23. *V. Baier, V. Katkov, V. Strakhovenko*. ZhETF, 92 (1987) 1228.
24. *I. Ginzburg, G. Kotkin, S. Polityko*. Yad. Fizika, 37, vyp.2, (1983) 368.
25. *I. Ginzburg, G. Kotkin, S. Polityko*. Yad. Fizika, 40, vyp.6 (12) (1984) 1495.
26. *L. Landau, E. Lifshits*. Kvantovaya Mekhanika, M.: Nauka, v.1.
27. *V. Parkhomchuk*. Private Communication.
28. *I. Ginzburg, G. Kotkin, S. Panfil, V. Serbo*. Nucl. Phys., B228 (1983) 285.
29. *J. Ellis*. Proc. of Sum. Inst. on Part. Phys., 1978, SLAC-215.
30. *L.B. Okun*. Leptons and Quarks. M.: Nauka, 1981 (in Russian).
31. *F. Schrempp*. DESY 85-006 (1985).
32. *G. Kotkin, S. Polityko, V. Serbo*. Yad. Fiz. 42 (1985) 692.
33. *N. Klepikov*. ZhETF, 26 (1954) 19.
34. *T. Erber*. Rev. of Mod. Phys., 38 (1966) 626.
35. *V.N. Baier, V.M. Katkov*. ZhETF, 53 (1967) 1478.
36. *V.N. Baier, V.M. Katkov, Strakhovenko*. Electromagn. Processes at High Energy in Oriented Crystals. Novosibirsk: Nauka, 1989 (in Russian).
37. *P.Chen*. Summary Talk at Intern. Workshop on the Next Generation Linear Colliders, December, 1988, SLAC.
38. *P. Chen, V.Telnov*. SLAC-PUB-4923 (1989), Phys. Rev. Lett, 63 (1989) 1796.
39. *R. Blankenbecler and S. Drell*. SLAC-PUB 4810.
40. *R.B. Palmer*. SLAC-PUB-4707 (1988).
41. *J.C. Sens*. Proc. of the VIII Inter. Workshop on Photon-Photon Collisions, April, 1988, Israel.

*V.I. Telnov*

**Problems of Obtaining  
 $\gamma\gamma$  and  $\gamma e$  Colliding Beams  
at Linear Colliders**

*В.И. Тельнов*

**Проблемы создания  
встречных  $\gamma\gamma$ - и  $\gamma e$ -пучков  
на линейных коллайдерах**

Ответственный за выпуск С.Г. Попов

---

Работа поступила 9 июня 1989 г.  
Подписано в печать 16.06.89 г. МН 10278  
Формат бумаги 60×90 1/16 Объем 3,7 печ.л., 3,0 уч.-изд.л.  
Тираж 180 экз. Бесплатно. Заказ № 91

---

*Набрано в автоматизированной системе на базе фото-наборного автомата ФА1000 и ЭВМ «Электроника» и отпечатано на ротапинтере Института ядерной физики СО АН СССР, Новосибирск, 630090, пр. академика Лаврентьева, 11.*